8-2010

Design, fabrication, and testing of a microfluidic system for cardiac cell culture.

Mai-Dung Thi Nguyen
University of Louisville

DESIGN, FABRICATION, AND TESTING OF A

MICROFLUIDIC SYSTEM FOR CARDIAC CELL CULTURE

By

Mai-Dung Thi Nguyen

B.S., the University of Oklahoma, 1999

A Thesis

Submitted to the Faculty of the

Speed School of Engineering, University of Louisville

in Partial Fulfillment of the Requirements

for the Degree of

Master of Science

Department of Mechanical Engineering

University of Louisville

Louisville, Kentucky

August 2010

DESIGN, FABRICATION, AND TESTING OF A

MICROFLUIDIC SYSTEM FOR CARDIAC CELL CULTURE

By

Mai-Dung Thi Nguyen

B.S., the University of Oklahoma, 1999

A Thesis Approved on

June 17, 2010

By the following Thesis Committee:

_____

Dr. Palaniappan Sethu, Thesis Director

_____

Dr. Cindy Harnett

_____

Dr. Thomas Berfield

_____

Dr. Guruprasad Giridharan

DEDICATION

This thesis is gratefully dedicated

to my lovely deceased aunt, Say Nguyen,

my family: grandmother, parents, brothers, sister-in-law, and nephew,

and

the Dominican Sisters of Peace and Associates

ACKNOWLEDGMENTS

ABSTRACT

DESIGN, FABRICATION, AND TESTING OF A

MICROFLUIDIC SYSTEM FOR CARDIAC CELL CULTURE

Mai-Dung Thi Nguyen

June 17, 2010

Cardiovascular disease (CVD) is the leading cause of death in the United States and accounts for nearly 1,372,000 deaths each year. In addition, ~ 81 million Americans suffer from some form of CVD. Understanding the molecular basis of various manifestations of CVD requires cellular-level studies. However, current technologies for cell culture, fail to recreate the *in-vivo* environment where cells are subject to pressure and stretch as a consequence of normal hemodynamic loading and unloading. Therefore, to study cardiac cells with physiological relevance, the mechanical loading environment needs to be accurately replicated *in-vitro*. In order to create an appropriate platform for cardiac cell culture, a microfluidic cardiac cell culture model (µCCCM) was designed and fabricated. This system consists of a pump, cell culture chamber, pneumatically actuated collapsible valve and a tunable resistance element in series. By varying the pump flow rate, valve closure frequency and the outflow resistance, various conditions associated with normal and dysfunctional heart function were recreated. A rat left ventricle heart muscle cell line (H9c2) was used to establish proof-of-concept and

demonstrate the ability of the μCCCM to sustain cell culture under normal physiological conditions. Microscopic evaluation of these cells using phase contrast and immunofluoresence demonstrated that cells cultured within the μCCCM achieved an *in-vivo* like phenotype in comparison to static unloaded controls.

Keywords: microfluidics, cardiac, fabrication, cardiovascular disease, heart failure, PDMS thin membrane.

TABLE OF CONTENTS

LIST OF TABLES

LIST OF FIGURES

CHAPTER I- CARDIOVASCULAR DISEASE AND THE HEART

1.1. CARDIOVASCULAR DISEASE (CVD)

The cardiovascular system consists of the heart, blood vessels (arteries, capillaries, and veins) and blood. The heart acts as a pump to circulate blood through the lungs to oxygenate, and flow through arteries to deliver oxygen and nutrients to the entire body. When the blood is delivered to tissues, the oxygen and carbon dioxide are exchanged . The deoxygenated blood is then returned to the heart via veins and finally to the lungs, helping dispose carbon dioxide and other waste products.

CVD collectively refers to abnormalities associated with various components of the cardiovascular system and covers over 60 disorders relating to the heart and vascular system. CVD is the leading cause of death in the United States and claims ~ 1,372,000 lives each year [1-3] which is higher than the next 4 leading causes of death combined. Statistics from the American Heart Associate (AHA) indicate that ~ 81 million people or $1/4^{th}$ of the population suffers from some form of CVD in the United States. This includes high blood pressure ~ 74.5 million; coronary heart disease ~ 17.6 million; stroke ~ 6.4 million; congenital cardiovascular defects ~ 650,000 to 1.3 million; and heart failure ~ 5.8 million.[1-2, 4] Based on the article: "Heart Disease and Stroke 2010 Update" from AHA, it is estimated that the total indirect and direct cost due to CVD and

stroke in 2010 will be ~ 503.2 billion dollars placing a severe burden on the economy and diminishing the quality of life for several thousands of people. [5-6]

CVD can be classified into two major categories based on disorders of the heart or the vascular system. Disorders of the heart include conditions such as angina pectoris, arrhythmias, cardiomyopathy, congestive heart failure, and congenital heart disease. Disorders of the vascular system on the other hand include conditions such as aortic aneurysms, arteriosclerosis, high blood pressure, stroke, and transient ischemia. [4] Coronary heart disease is the most common type of CVD. It is a condition which fatty deposits build up inside the inner walls of coronary arteries, creating blockages of the arteries. These blockages reduce the blood flow, causing a pain or discomfort in the chest, heart failure (HF) and heart attacks. Similar to the coronary heart disease is atherosclerosis. In this disease, the arteries become thicker or harden; and the inner wall of the arteries becomes narrower due to the deposits of fat, cholesterol or other substances. This narrowed passage can block the blood flow and lead to heart attacks and strokes. Strokes occur when the blood vessels to the brain are occluded or broken. As a result, brain cells begin to die due to lack of oxygen and nutrition.[5-6] Stroke usually relates closely to high blood pressure, which happens when the pressure inside the vessels is higher than the normal range, which is about 120/80 mmHg. High blood pressure can cause HF, stroke, kidney failure, or other health problems.[7] The end stage for different CVDs is HF (Fig.1.1) which occurs when the heart fails to pump sufficient blood through the body. The body, therefore, does not get enough oxygen and nutrients. HF develops slowly over time; and if not treated, can cause life-threatening conditions including

pulmonary edema, failure of brain, kidney and other major organs, and myocardial infarction.

```
                    ┌─────────────────┐
                    │  Initial Injury │
                    └─────────────────┘
                             ↓
┌──────────────────────────────────────────────────────┐
│   Body regulation system responds for compensation    │
└──────────────────────────────────────────────────────┘
                             ↓
┌──────────────────────────────────────────────────────┐
│          Heart rate and blood pressure rise           │
│                   Arteries constrict                  │
│ .... Eventually, the heart structure deforms/remodels │
└──────────────────────────────────────────────────────┘
                             ↓
┌──────────────────────────────────────────────────────┐
│ Gradually, these changes promote circulatory congestion│
│            and increase strain on the heart            │
└──────────────────────────────────────────────────────┘
                             ↓
            ┌───────────────────────────────┐
            │        Heart weakened         │
            │             and               │
            │    poor pumping performance   │
            └───────────────────────────────┘
                             ↓
                ┌───────────────────────┐
                │     Heart Failure     │
                └───────────────────────┘
```
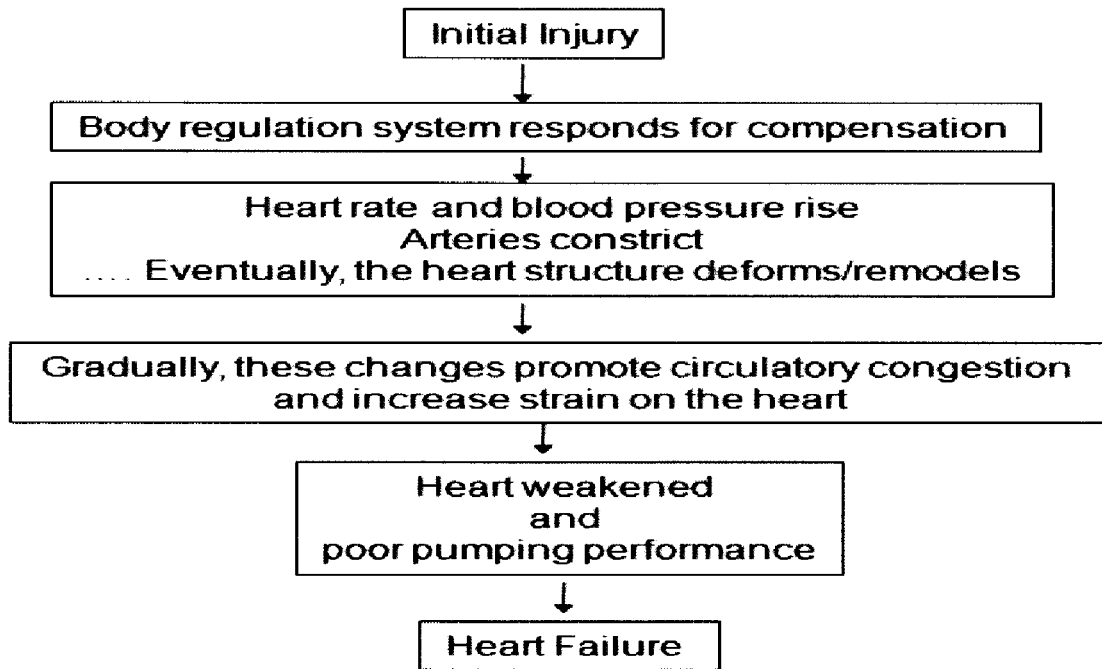
Figure 1.1. Heart Failure is the end-stage of dysfunctional cardiovascular system existing for a long term.

1.2. TREATMENT OF HEART FAILURE

HF is a chronic disease; therefore, the treatment for HF needs lifelong management, which includes changes in living habits, medication, and assist devices to augment heart function. [8-9] The only cure for end- stage heart failure is total heart transplantation.

Drug therapy is usually used for the initial stage of the HF. Depending on the stage and symptoms of HF, a single or combination of different medications are applied. The most common drugs used for treatment of HF include Angiotensin-converting enzyme (ACE)

inhibitors or Angiotensin II receptor blockers (ARBs), Digoxin (Lanoxin), Beta blockers, Diuretics, and Aldosterone antagonists.[10] Angiotensin-converting enzyme (ACE) inhibitors or Angiotensin II receptor blockers (ARBs) dilate the arteries and improve blood flow, therefore, decrease the workload on the heart. Digoxin (Lanoxin) helps to strengthen the contraction of heart muscle and slow the heart beat. Beta blockers reduce the heart rate and pressure. [10-11] Diuretics enhance urination frequency to keep from the fluid building up in the body, especially in the lung. Aldosterone antagonists help the heart work better.

When the HF advances to a more serious stage, assist devices may be also used for the treatment. For example, implantable cardioverter-defibrillators are used for monitoring the heart rhythm. Cardiac resynchronization therapy or biventricular pacing are used to help the heart pump efficiently by sending timed electrical impulses to the heart's ventricles for contraction. Left ventricular assist device (LVAD) is used in a short term to assist those who are waiting for heart transplant or in a long term treatment for those have a weakened hearts or HF but cannot get a heart transplant.[12] LVADs are designed as mechanical pumps to transport blood from left ventricle to the body.

Heart transplant is applied for those who reach the end-stage of the HF. A healthier heart from a donor is replaced for the failing diseased heart.[13] However, people undergoing heart transplant face high risk of the rejection of the donor heart, infection, artery problems, medication side effect and potential high risk of cancer due to the

immunosuppresant medications.[13] In addition, due to the shortage of donors, people who need heart transplants experience long wait times.

Heart transplant or LVAD are currently the only options for the end-stage HF. However, due to the lack of donors and the complications associated with immunosuppressive treatment as well as many high risks occurred during surgery, scientists and surgeons continue to search for new strategies to treat the HF.

1.3. THE HEART

The heart, through one organ, functions as two pumps coupled to one another in series. The right pump receives deoxygenated blood from entire body and pumps it to the lungs for oxygen-carbodioxide exchange while the left pump receives the oxygenated blood from the lung and then delivers this oxygenated blood to the entire body. As the result, the pressure in the right pump is lower than in the left pump. However, to perform pumping function, both the left and right pump needs to match their output volume.

1.3.1. Gross anatomy of the heart

Each side of the heart has a main pumping chamber (the ventricle), the holding chamber (the atria) and two valves to prevent back flow (Fig. 1.2.). The valve between the right atria and right ventricle is the tricuspid valve and between the left atria and left ventricle is the mitral valve.[14-15] These valves prevent the flow of blood back into the atrium when the ventricles contract. Pulmonic valve and aorta valve in the right and left ventricle prevent the blood from pulmonary artery and aorta flowing back to the right and

left ventricle when these ventricles relax. The two ventricles share a common wall and electrical system to stimulate and control the pump function.
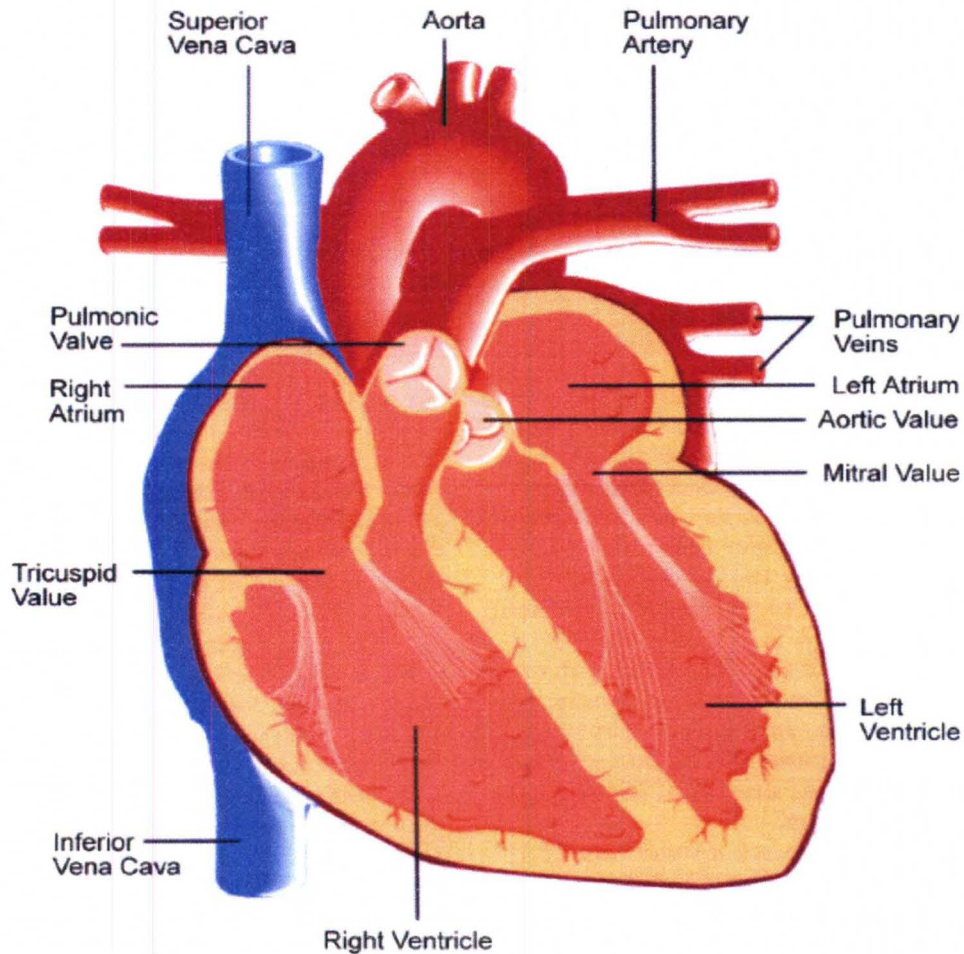
Figure 1.2. Gross anatomy of the heart.

(*http://www.emedicinehealth.com/slideshow_heart_disease/article_em.htm*)

Deoxygenated blood from the vena cava system flow back to the heart and is held in the right atria. When the tricuspid valve opens, the blood flows into the right ventricle. The blood in the right ventricle is pumped to the lung. Through the pulmonary artery, the oxygenated blood is brought to the left atria and then poured to the left ventricle when the

mitral valve opens. The left ventricle pumps the blood into the aorta to deliver blood throughout the body. Due to the pressure in the aorta being much higher than the pulmonary system, the left ventricle needs more force to pump; therefore, the muscle wall of the left ventricle is thicker than the right one. The walls of the atria are also much thinner than the ventricles.[14-15]

1.3.2. Cellular organization

Cardiac tissue is composed of three different major cell types: cardiomyocytes, cardiac endothelial cells, and smooth muscle cells.[13-15] Cardiomyocytes are the cells that make up the heart muscle and have the ability to contract spontaneously. To perform their function in synchrony, cardiomyocytes need to align in parallel and establish end to end cell-cell contacts (Fig.1.3.). Smooth muscle cells form a contiguous layer over the cardiomyocytes and finally a layer of endothelial cells line the myocardium providing shear protection. Besides these major cell types, cardiac tissue are also composed of cardiac fibroblast. Cardiac fibroblasts relate to heart remodeling, therefore, play a critical role in heart hypertrophy and heart failure. [16]

1.4. WORKING OF THE HEART

Heart, consists of two atria and two ventricles, is the organ responsible for pumping blood throughout the body. The tension inside the heart due to the blood loading sends the mechanical then electrical signals inside the cells. This electrical signals travel through signal transduction pathway to stimulate the heart to pump. In response to this,

the chambers of the heart contract rhythmically, first both atria, then the ventricles. The working principle of the right pump side is similar to the left pump.

Figure 1.3. Arrangement of cardiomycocytes in the cardiac muscle.
(http://www.brown.edu/Courses?BI0032/adltstem/cardiac-muscle.gif)

A pump cycle of the heart for the left pump can be also divided into two main periods: the systolic and diastolic periods. The systolic period starts when the mitral valve closes and muscle begins to contract until the aortic valve close after the blood in the ventricle is ejected to the aorta. The diastolic period starts when the aortic valve closes and the muscles begin to relax until the mitral valve closes after filling the blood from the atrium to the ventricle.[14-15, 17]

The relationship between pressure and volume, the pump cycle of the heart especially for the left ventricle chamber can be divided into four phases: the ventricular filling or

8

diastole, the isovolumetric contraction, the ejection, and isovolumetric relaxation (Fig.1.4.). [14-15, 17-18] During the ventricular filling phase, the relaxation of the heart muscles reaches to the maximum level. Therefore, when the blood from the atria continues to fill in the ventricle, the pressure of the ventricle goes up gradually and the blood volume is increased significantly, which is represented by phase 'a' on the pressure-volume loop. When the ventricle pressure reaches a certain level, the muscles contract.[18] The pressure in the ventricle at this point is higher than the atria, the mitral valve closes, but this pressure is not sufficient to open the aortic valve. Because all valves are closed, the pressure is increased dramatically while the volume remains the same, which is called the isovolumetric phase (phase b). At this point, the ventricle begins to contract until the pressure inside the ventricle chamber exceeds the aortic diastolic pressure; then the aortic valve opens, starting the ejecting phase (phase c). Once the aorta valve is opened, the blood inside the left ventricle is ejected to the aorta, causing a decrease in volume. However, the pressure still keeps increasing until it reaches to its peak, then decreases when the ventricle begins to relax, causing the closure of the aorta valve due to the pressure in the aorta larger than in the ventricle. In this relaxation, because of the closure of valves, the pressure inside the ventricle goes down quickly while the volume remains unchanged, creating a vertical line on the diagram B on the figure 4. When the pressure inside the left ventricle (LV) is lower than the left atria pressure, the mitral valve opens and the LV is filled with blood. At this point, the LV relaxes causing the pressure continues to fall. Once the relaxation of the LV stops, the pressure gradually increases when the volume increases.[14-15, 17-18]

9

A

Phase

a b c d a

Aortic
Valve
Opening

Aortic
Valve
Closing

Mitral
Valve
Closing

Mitral
Valve
Opening

100

LVP
(mmHg)

100

LVVol (ml)

0

EDV

ESV

Time

B

The aortic valve
closes

The aortic valve
opens

100

LVP (mmHg)

c

d

b

The mitral valve
opens

a

The mitral valve
closes

0

0   50   100   150

LV Volume (ml)
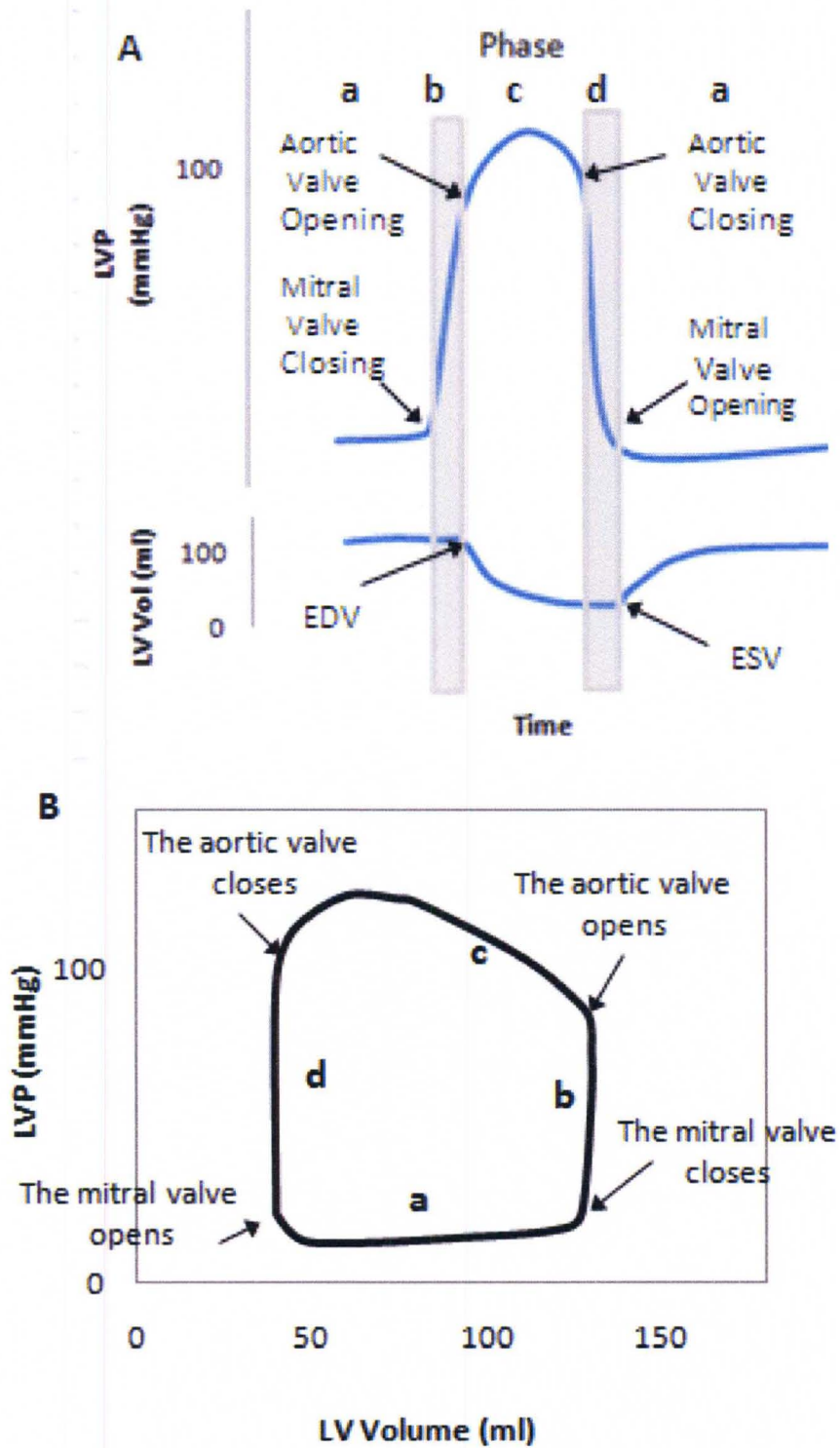
Figure 1.4. Relationship between pressure and volume during the pump cycle of the heart. (A) Cardiac cycle diagram and (B) Pressure-Volume Loop. (a) Refilling phase, (b) Isovolumetric phase, (c) ejecting phase, and (d) Isovolumetric.

In normal condition, human heart rate is about 70±10 beats per minute (bpm), the stroke volume is about 60±10 mL/beat, left ventricular systolic peak pressure approximates of 120±10 mmHg; and left ventricular end diastolic pressure ranges from 5-12 mmHg. [19-20]. Stroke volume is the volume of blood ejected for each beat.

1.5. CELLULAR RESPONSE TO MECHANICAL SIGNALS

When a mechanical stimulus is applied to the extracellular matrix (ECM), the cells detect this mechanical stimulus via mechanoreceptors such as integrins. These mechanoreceptors are located in the plasma membrane connecting the extracellular and intracellular regions of the cells, traducing the mechanical signals from outside to the inside the cell.(Fig.1.5.).[17, 21]   Once the signal is transmitted inside of the cell, the signal triggers biochemical changes via signaling transduction pathway, enhances the formation of sarcomere, and alters directly the structure of the cytoskeleton.[17, 21]

In cardiovascular system, two important signal transduction pathways are known: G-protein and inositol triphosphate (IP$_3$) pathways.[21] In the heart, the mechanical signals activate G-proteins to bind to the cell receptors. This binding complex activates the formation of cyclic AMP (cAMP); as a result, the concentration of Ca^{++}inside the cell increased (via ion channels or from sarcoplasmic reticulum). [21] The increasing of Ca^{++} promotes the contractility of the cardiomyocytes.[22] In IP$_3$ pathway, once stimulated by mechanical signals, cell surface receptors bind to G$_q$ proteins, enhancing the formation of inositol triphosphate IP$_3$. This IP$_3$ formation promotes the release of Ca^{++} inside the cells,

which increases the contractility.[21] Therefore, any disorder on these pathways can alter the contractile ability of the heart muscle.
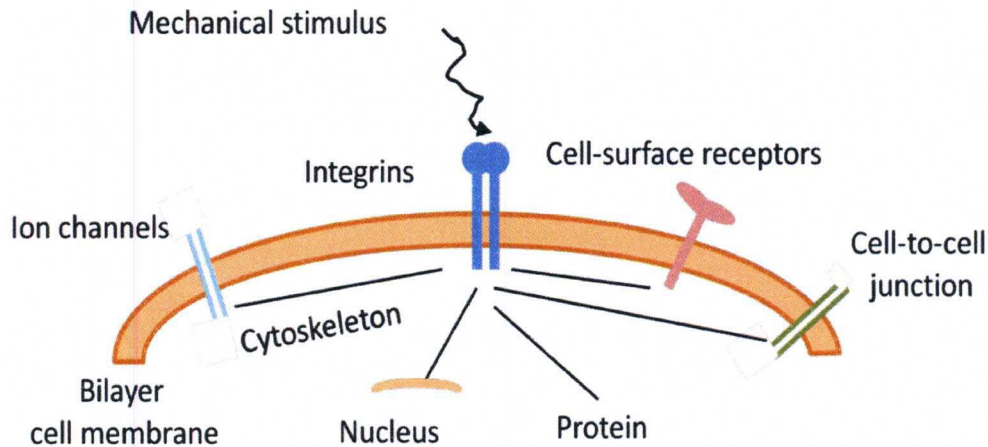
Figure 1.5. Transduction of mechanical stimulus at the cellular level.

The length of sarcromere, a basic contractile unit of cardiomyocyte, is also affected by the mechanical stimulation.[23] When the muscle is stretched to a length greater than normal size, new sarcomere units are added rapidly at the end of the muscle fibers.[22, 24] Unlike the skeletal muscle, sarcomere length in cardiac muscle does not change very much, and small change in sarcomere length can result large changes in tension generation.[23, 25-26] Therefore, increasing the sarcomere length enhances the tension development, which affects the changes both in preload condition and the contractility of the heart.

In addition, the deformation of the cytoskeleton can change the physical properties of the cells and distort the nucleus, as well as the biochemical and molecular events inside the cell, such as gene expression, transcription, translation and protein synthesis. This

change also affects physical and chemical communication between cells. Therefore, the structure inside the cell and the morphology of cell as well as the biochemical aspects of the cell are altered as a result of mechanical stimulus.

To respond to these changes, the heart begins to remodel itself. The remodeling of the hearts causes to increase the number of fibroblasts, thickens the heart muscle wall, or enlargers the size of the hearts.[24, 27-28] These changes play critical roles in contractility of the cardiac tissue. If the mechanical stimulus insists, these modification of the heart can lead to the HF (Fig. 1.6)
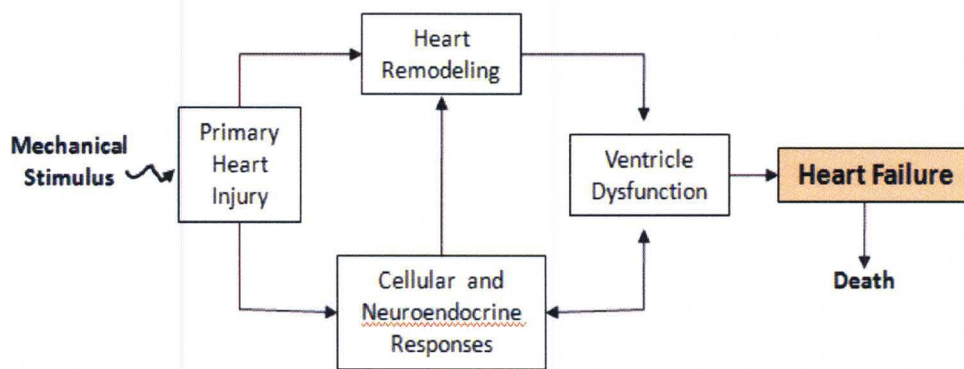
Figure 1.6. Physiological responses due to mechanical stimulus leading to heart failure.

1.6. CONCLUSION

CVD is a serious health problem and continues to claim several lives each year while also diminishing quality of life for several others. Current treatment options, though beneficial have several limitations. The heart is the central organ within the cardiovascular system and is extremely complex in terms of construction and function. This chapter serves to provide an overview of CVD and the heart structure and function.

CHAPTER II- *IN-VITRO* MODEL SYSTEMS TO STUDY CARDIAC TISSUE

2.1. NEED FOR CELLULAR-LEVEL STUDIES

The human body consists of various levels of internal organization. Cells are the smallest functional units capable of sustaining themselves. Cells consist of various molecular constituents including bio-molecules like DNA, RNA and proteins. Cells are organized together to form tissue. Organs in the body responsible for specialized functions are made up of one or more types of tissue. Various organs and/or tissue in the body are organized together to form systems (Ex: Cardiovascular, Nervous, or Circulatory). Finally, an organism sustains life due to synergistic working of various systems within the body. Several mechanisms exist to provide feedback and maintain the body's functions within a tight range (homeostasis).

The tradeoff between generation of highly specific molecular information and translation of that information *in-vivo* necessitates investigation at various levels of cellular organization (Fig. 2.1). Cell based studies are essential to provide highly specific information relating to molecular mediator and the targets for drug discovery and therapy. Analysis of purified or isolated cell populations free from surrounding cellular and extracellular constituents allows the investigation of sub-cellular mechanisms in great detail not possible in intact tissue.[29] Study of heterogeneous mixtures of cells (like in

14
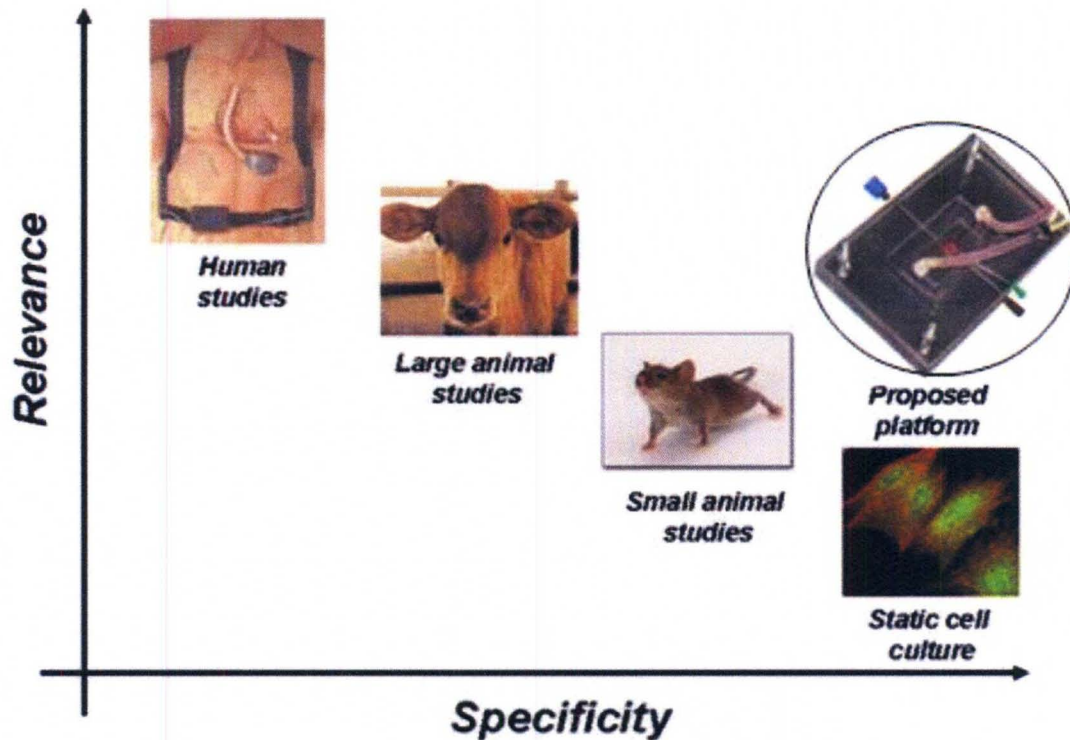
Figure 2.1. Specificity vs. Relevance plot. Human clinical studies are the most relevant but least specific whereas cellular level studies provide highly specific information but their relevance to human physiology is low. The µCCCM seeks to significantly enhance the relevance of cellular level studies.

tissue) often results in unnecessary noise which significantly deteriorates the quality of information attainable. Further, cellular level systems that utilize purified cells, allow for convenient analysis using both destructive and non-destructive techniques. Cells can be imaged using microscopy to study structure, conformation, the expression of intra- and extra-cellular markers, organization of organelles and other details of nuclear and cytoskeletal elements. Low and high- throughput techniques can be used to evaluate gene expression, protein expression and production of metabolites. The effect of a drug or therapeutic can be understood in terms of molecular signaling events that alter cell

15

phenotype and function. High-throughput cell culture using multi-well plates can be used to evaluate effects of variables including concentration of stimulants and time of exposure on cellular function.[30] The flexibility and specificity of information generated from cellular level systems is unparalleled and is usually an essential first step in any drug discovery study. However, since cell based studies use isolated cells in a non-physiological environment without mechanisms responsible for homeostasis, the relevance of these studies is limited and results need to be verified using animal and patient level studies.

In-vitro studies are performed in isolation without feedback mechanisms present in the body. Therefore, to understand the real and long term effects of a biochemical compound, drug or device on an organ, a system, *in-vivo* evaluation is essential. Animal studies are used to confirm outcomes before application in the human body. Animals are similar in complexity to humans and the levels of organization are conserved amongst most species. Small animal studies are easier to perform due to cost related issues and availability of significant amount of information and characterization of various systems in animals like rats, mice, hamsters and rabbits.[24, 31] Further, technologies for generation of transgenic animals allows for greater flexibility with design of studies to evaluate targeted pathways.[32] Large animals are physiologically closer to humans and provide improved relevance due to greater similarities in size of organs and function of systems.[33-34] Large animals are particularly useful in testing implantable medical devices as the size of organs is comparable to humans and provides a more accurate representation of the actual situation.

Patient or clinical studies are often the last stage of evaluation for a particular drug or treatment. This follows pre-clinical studies accomplished using *in-vitro* methods and *in-vivo* animal studies. Clinical trials allow assessing the safety and effectiveness of a new medicine or device on patients. Clinical studies are divided into phases 0, 1, 2, 3, and 4. Phase 0 trial allows an early evaluation of the pharmacological effect of the testing drug in humans This is done by administrating a low dose of the test compound in a short time period. This phase 0 trial doesn't have atherapeutic or treatment purpose; rather, allows the researchers to explore the pharmacological profile of the test compound in human to see if it is appropriate for humans or not.[35] As a result, it helps to select the potential drug. The disadvantage of this phase is the poor relation between the preclinical and clinical effect of the testing drug.[36] Phase 1 is the first stage to test the dose effects on human subjects, so the appropriate dose of a certain drug on human can be found. Phase 2 trials assess how well the drug works and continue to affirm the safety of the drug on large groups. Phase 3 trials are applied on a huge group to see how effective the drug is for a certain type of disease. And finally, phase 4 relates to the on-going effect of the drug.

In conclusion, cell-level studies are highly specific and can be used to investigate molecular mediators and signaling pathways involved in disease processes. These studies cannot be accomplished in patients because of inherent difficulties with isolation of cells and analytical techniques. Animals provide a more appropriate platform for early evaluation as they provide more opportunities for evaluation. To shorten the time between discovery and clinical validation, it is essential that cell based studies are

accomplished in platforms that have physiological relevance. For example: studying cardiac tissue under unloaded static conditions is undesirable since mechanical loading and fluid flow play an important role in maintaining cell structure and phenotype.

2.2. IMPORTANT CONSIDERATIONS FOR CELL-LEVEL METHODS OF CARDIAC TISSUE

During normal heart function, the myocardium experiences passive stretching and pressure build-up during filling (preload) and actively generates mechanical force during ejection (contraction) against variable afterload. Cells in cardiac tissue therefore are under constant physical stimulation and rely on conversion of these cues into intracellular signals to control cell phenotype and muscle mass during conditions,[37] such as hypertrophy. Cardiac cells therefore are exposed to periodic pressure, stretch and shear stress.

Physiological heart development and cardiac function rely on the response of cardiac tissue to mechanical stress signals during hemodynamic loading and unloading. These stresses manifest themselves via changes in cell structure, contractile function and gene expression.[31] Disruption of this well-balanced stress-sensing machinery due to various pathological conditions results in mechanical dysregulation, cardiac tissue remodeling and heart failure. To achieve physiological relevance, *in-vitro* models must replicate the complex, dynamic *in-vivo* interactions between cardiomyocytes and mechanical stress signals. Current *in-vitro* models do not incorporate all aspects of mechanical loading and therefore fail to accurately mimic the *in-vivo* cardiac microenvironment.

2.3. CURRENT STATE OF THE ART

Despite advances in isolation and culture techniques, the current state of cardiovascular *in-vitro* models is predominantly based on glass slides or tissue culture dishes under static conditions.[28-29, 38] Most studies utilize isolated cells maintained in two-dimensional culture forming randomly oriented cell -ECM attachments.[32, 39-40] Accurate replication of the *in-vivo* environment requires consideration of several factors. First, tissue orientation and direction of stretch are critical determinants of cardiac cell signaling; therefore randomly oriented cultures cannot replicate physiological loading. Second, fluid flow is an important determinant as shear stress strongly influences endothelial and smooth muscle phenotype; hence, perfused systems are more representative of the *in-vivo* environment. Third, cyclic build-up of pressure and stretch during preloading are critical determinants that dictate cell structure and function. Fourth, synchronous contractions that enable unloading, ensures ejection of fluid that in turn results in relaxation of built-up pressure and stretch.[16]

Some of the aforementioned issues have been previously addressed, albeit individually. Patterning of ECM proteins using techniques like micro-contact printing and lithography to define areas of cell attachment and directional alignment have been accomplished.[41-43] Several groups have reported culture of cardiac cells under conditions of perfusion using continuous and cyclic loading to mimic *in-vivo* hemodynamic loading.[44-47] Mechanical stretch simulating hemodynamic loads are studied using technologies like Flexcentral Flexercell® Strain - FX-4000 Flexercell Tension Plus [TM] (*http://www. flexcellint.com*) which consists of a flexible membrane on which cardiac cells can be

19

plated and then be subject to oscillatory deflections using a vacuum or pressure source.[48-49] Electrophysiological studies utilize systems like IonOptix Myocyte Systems (*http://www.ionoptix.com*) where cardiomyocytes grown on a glass slide are stimulated with an electrical impulse and analyzed for contractility via fluorescence using hardware and software developed by the manufacturer. However, to the best of our knowledge there is no system currently available that recreates all aspects of cardiac mechanical loading.

2.4. PHYSIOLOGICALLY RELEVANT SYSTEMS FOR CARDIAC CELL CULTURE

Various manifestations of cardiovascular diseases directly correspond to changes in mechanical behavior of cardiac cells. This in turn affects cellular phenotype and function, causing changes like hypertrophy, growth of fibrous tissue, and establishment of random cellular orientation.[28] For example, in hypertension, the pressure inside the heart exceeds the normal range due to a high resistance in vascular system and results in hemodynamic overloading of the heart. This higher pressure dilates the cardiomyocyte cells.. In the long term, this additional stretch weakens the ability to the contraction of heart muscle, causing heart failure.[24] In the contrast, hypotension refers to the condition where the pressure inside the heart is lower than the normal range. This causes reduced blood circulation and oxygen deprivation to the rest of the body. In response to this oxygen shortage, the heart rate is increases resulting in altered stretch and pressure profiles.

The frequency of the loading determines the ranges for normal and abnormal heart function. For example, bradycardia is a condition where the heart rate is lower than 60 bpm [50] and tachycardia is another condition characterized by significantly higher heart rate (>200 bpm) in comparison to normal heart rate (~75 bpm). In response to these abnormal patterns, the heart either lowers or increases the systolic fraction.[51] All of these changes can cause the reorganization of cardiac tissue and it can lead to heart failure or sudden death if it persists long term.[15]

Finally, shear stress due to fluid flow can be a significant determinant for cardiac endothelial and cardiac smooth muscle cells. Cardiac endothelial cells contribute to the internal lining of the myocardium and are directly exposed to fluid induced shear stress during hemodynamic loading and unloading. Changes in magnitude, frequency and duration of shear stress are a critical determinant of endothelial cell structure, function and permeability. Various clinical conditions result from changes to shear profiles seen by cardiac endothelial cells.

Studying cardiovascular disease requires appropriate cellular level platforms which can be used to culture cells while accurately mimicking mechanical and fluidic loading conditions seen *in-vivo*. In cardiovascular disease, various conditions are associated with distinct mechanical loading profiles and replication of those profiles is critical to ensure proper understanding at the cellular and molecular levels. Mechanical loads experienced by cardiac cells that vary as a consequence of dysfunction include pressure, stretch and shear as well as the frequency and duration.

In conclusion, based on the discussion above, due to the complex nature of the heart and the importance of mechanical loads, a cellular culture model with physiological relevance is critical to investigate the cellular and molecular basis of cardiovascular disease. No device or cell culture platform available today has accomplished long term culture of cardiac cells *in-vitro* with accurate replication of mechanical loading profiles. Efforts by other groups thus far have succeeded in replicating isolated mechanical loads. There is still a need for platforms where the culture conditions can be dynamically varied to not only replicate normal loading conditions, but also abnormal loading conditions. These platforms are necessary to study the molecular pathophysiology of cardiovascular diseases and in the discovery of drugs, treatment options and cardiac cell regeneration strategies.

CHAPTER III- DESIGN AND FABRICATION OF THE μCCCM

3.1. MECHANICAL LOADS IN THE HEART

The magnitude and duration of stretch and contractions in cardiac tissue depend on the preload and afterload conditions. In the heart, specifically in the left ventricle, preload refers to the condition when the filling of blood inside the ventricle causes the stretch of the wall during the diastolic phase. Afterload refers to the resistance in the system that needs to be overcome to pump blood out of the ventricle via opening of the aortic valve.[15] This directly affects the contractile force that needs to be generated by cardiomyocytes. Overcoming this pressure opens the aortic valve for ejecting the blood into the aorta.

Preload increases when blood filling the chamber during diastole increases, which creates greater systolic pressure for the subsequent contractions. This systolic pressure continues to increase until its maximum systolic pressure is reached at the optimal preload. At a constant preload, through the ventricular contraction, higher systolic pressure can be obtained by raising the afterload condition such as increasing the aorta pressure.[15] However, if the afterload keeps increasing, the ventricle cannot create enough force to open the aortic valve to push the blood out of the heart. At this point, the systolic phase is totally isovolumetric. Preload and afterload, as a result, depend on the vascular system

and the behavior of the heart including peripheral resistance, the frequency of the heart's contraction, and change of the stroke volume.[15]

3.2. *IN-VITRO* TECHNIQUES FOR MECHANICAL STIMULATION OF CELLS

There are different ways to mechanically stimulate cells in *in-vitro* culture to replicate effects of physiological levels of preload and afterload.[17] These include:

Compressive Loading

Stretch

Fluid flow

Cells in different tissue experience compressive loads due to pressure buildup. Cardiac and vascular tissue are examples of tissue where cells within the tissue are constantly under compressive loading. Replicating this condition *in-vitro* can be accomplished using different techniques such as application gas pressure (hydrostatic compression) directly to the culture system or through the fluid induced loading of the system (pressure loading).[17] These techniques cause direct application of pressure to cells in culture mimicking conditions seen *in-vivo*.

Another commonly seen loading condition in cardiac and vascular tissue is stretch. The most common approach to stretch the cells in culture is by growing the cell on a flexible surface and applying stretch on the surface where the cells are attached. The stretch can be either uniaxial or biaxial.[17] With the uniaxial stretch, the surface is either rectangular or square and is stretched in one direction either longitudinally to both ends or is bent/flexed in a four-point bending. With the biaxial stretch, the membrane is

24

circular and the edge of the membrane is fixed. The applied pressure deforms the membrane in both the radial and circumferential directions.[17, 52] However, the strain depends heavily on the location on the membrane, causing the cells on different locations to stretch differently. For example, cells seeded at the center will stretch more than those at the edges. As the result, it is extremely complicated to analyze the data and to interpret the cells behavior. To produce equi-biaxial strain, the membrane has to slide non-frictionally on a stable plane. On this plane, the stress distribution on the area of membrane where is supported by the plane is symmetrical, creating an isotropic and spatially constant strain.[17, 52-54]

Finally cells in different tissue experience shear stress as a consequence of fluid flow.[17] Shear stress is a key mediator of cells phenotype and controls alignment and establishment of cell-cell contacts important in the formation of tight junctions which are extremely important in ensuring low permeability in vasculature. The velocity as well as the pattern of the flow, laminar versus turbulent flow for example, can create different shear stress on the cells. Also, viscosity of the fluid is another factor that can increase or decrease shear stress on the cells.[17]

In cardiac and vascular tissue, all three of these loads are experienced simultaneously. Additionally changes in one or more of these loads have a cascading effect on the entire system. Therefore *in-vitro* models of cardiac tissue need to accurately mimic the combined effects of pressure, stretch and shear in a pulsatile fashion.

25

3.3. COMPONENTS OF THE μCCCM

The μCCCM was designed to mimic the functioning of the left ventricle in the heart. This system consists of a peristaltic pump, cell culture chamber, pulsatile actuated collapsible valve and a tunable resistance element in series along with accessories that include tubing, an oil chamber, a pressure generator, and a digital manometer.

The μCCCM, fabricated using standard soft-lithography techniques consists of a small (~1cm diameter) cell culture chamber on a thin silicone membrane. Continuous circulation of culture medium is maintained using a peristaltic pump. Downstream of the chamber is a collapsible valve actuated in a pulsatile fashion using a pressure generator. Closure of this collapsible valve leads to pressure build up in the chamber which in turn also leads to stretching of the thin membrane on which cells are cultured mimicking diastolic preloading in the heart. To ensure uniformity, a post is placed beneath the thin membrane such that during stretch, the portion of the membrane on which cells are cultured experiences uniform strain and the edges experience larger non-uniform strain (Fig. 3.1). A tensile ring is used to ensure that the cells do not grow on the edges of the membrane, but on the thin membrane area that rests on the post but. Lubricating oil is filled in the chamber beneath the cell culture area which contains the post such that there is friction-free sliding of the membrane on the post. Further to influence outflow resistance, a tunable homeostasis valve is placed downstream of the collapsible valve to mimic afterload. This system is programmable and can accommodate a wide range and different combinations of operating parameters. Fluid transport and shear stress can be controlled by setting the flow rates of the pump. Pressure buildup and strain can be

controlled via a combination of factors including fluid flow rate and operation of both valves. Strain is also a function of the thickness of the membrane on which cells are cultured.
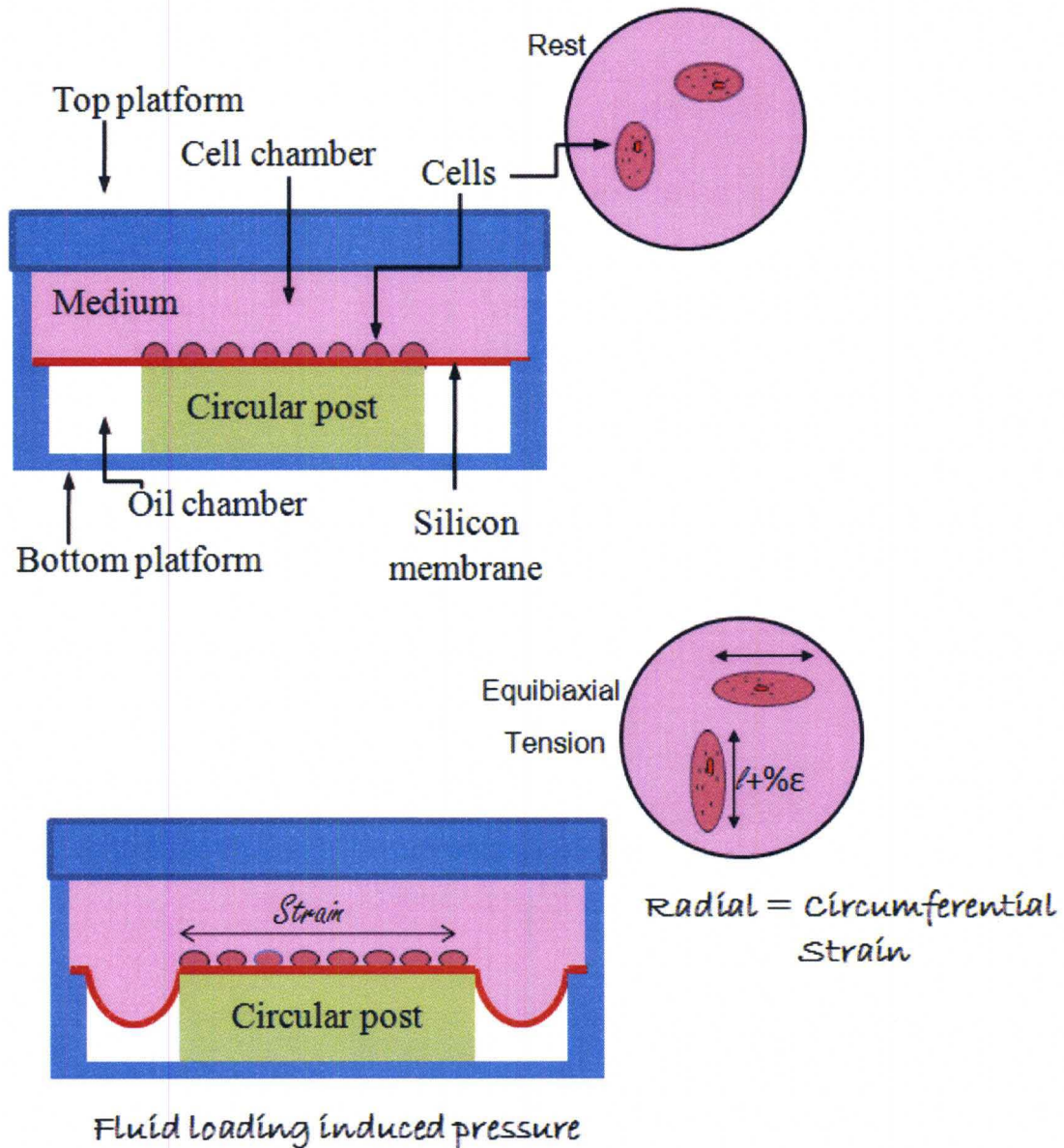
Figure 3.1. Setup design for equi-baxial strain. A significant deformation at the edges of the membrane occurs when the pressure is applied, but the area of the membrane rested on the post has the same radial and circumferential strain.

The μCCCM is unique in the sense that it mimics the native heart where changes in one or more variables have a cascading effect the entire system. For example, increasing the outflow resistance by manipulating the hemostatic valve indicates a system with high afterload. This in turn results in an increase in base pressure and baseline strain within the cell culture area mimicking conditions experienced during aortic stenosis or hypertension.

3.4. POLYDIMETHYL SILOXANE AS A MATERIAL FOR MECHANICAL STIMULATION

Polydimethyl siloxane (PDMS) is a pre-polymer: Sylgard 184 Silicon elastomer base and Sylgard$^{@}$184 silicone elastomer curing agent, manufactured by Dow Corning Corporation (Midland, MI). The PDMS rigidity can be controlled by the concentration of its cross-linker agent, the temperature, and the time of baking. The Young's modulus for PDMS is ~360-870 KPa with the density of 9.7 x 10-^{2} kg/m^3. Its fracture strength and poisson ratio are 2.24MPa and 0.49 respectively.[55]

PDMS is a substrate widely used for cell behavior studies because it is biocompatible and gas permeable. This silicone is also physically, chemically stable. PDMS also has a high flexibility and compressibility which is a good candidate for a thin stretchable membrane in μCCCM. PDMS material is also transparent; it is easy to monitor the fluid flow, to determine the functional integrity of fluidic circuits, or to check the cell behavior and structures under a microscope. In addition, PDMS is easy to mold or bond either to itself or to other materials including a glass slide; and is inexpensive. However, PDMS is

a highly hydrophobic polymer (contact angle is 90^0-120^0).[55] For the cells to attach and grow on it, PDMS membrane needs to be coated with ECM, such as fibronectin, laminin, or collagen.

3.5. DESIGN AND FABRICATION OF DIFFERENT COMPONENTS OF THE µCCCM

3.5.1. Assembly for Housing the Cell Culture Platform

The assembly for housing the cell culture platform was fabricated in the Rapid Prototyping Facility at the University of Louisville using Computer Numerical Control (CNC) Milling Machine. The designs were laid out using Solidworks 3D layout software prior to machining the assembly using CNC milling. Acrylic was used for construction.

This platform consists of identical top and bottom rectangular pieces (10.16 cm x 15.24 cm x 1.27 cm). The top piece has two half-circular channels (l = 2.54 cm, d = 0.38 cm) and two holes (d = 0.38 cm) at the outer ends of these two channels. (Fig. 3.2) The distance between two inner ends of these channels is 0.90 cm. The bottom part of the platform has two centric rectangular holes (7.62 cm x 5.08 cm x 0.64 cm and 5.08 cm x 2.54 cm x 0.64 cm). Finally, the platforms contain holes drilled all the way through at the corners for insertion of the screws.

3.5.2. Thin PDMS membrane

PDMS membranes were prepared by mixing 9.0 g of Silicon elastomeric base (Sylgard®184, Dow Conrning, Midland, MI) with 1.0 g curing agent for 1 minute.
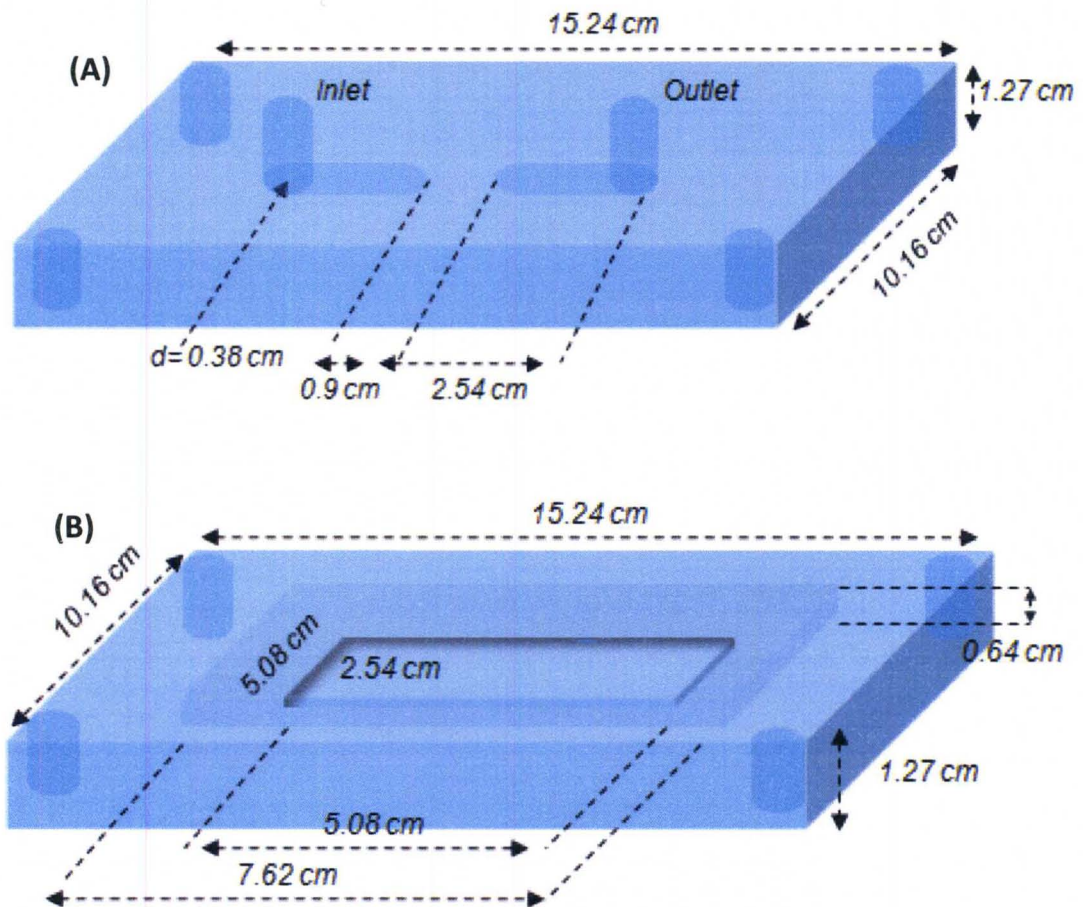
Figure 3.2. Schematic representation of the top and bottom pieces of the platform for housing the cell culture chamber. (A): the top part of the platform with inlet and outlet accesses and (B): the bottom part of the platform with two rectangular holes at the center.

Vacuum was then applied to the mixture to remove air bubbles created during the mixing. After 15 minutes, the remaining air bubbles on the surface were removed with a gentle stream of compressed air. Then, this mixture was used for thin membrane fabrication. Approximately 5.0 g of the degassed PDMS mixture was placed on a non-oxidized silicon wafer (0.525 mm thick, 100mm diameter, Silicon Valley Microelectronics, Inc. Santa Clara, CA) and spun at 400 rpm for 30 seconds on a Headway Spinner (Brewer Science, Inc., Rolla, MO) (See Appendix E for programming the spinner). The PDMS

coated wafer was then baked at 115 °C on a Standard Model 1100 Hotplate (Brewer Science, Inc., Rolla, MO) for 15 minutes. Once the PDMS was cured, the wafer was removed from the hotplate and cooled to room temperature. The membrane on the silicon wafer was then used for bonding to the cell chamber. The membrane thickness is a direct function of spin speed (Fig. 3.3).
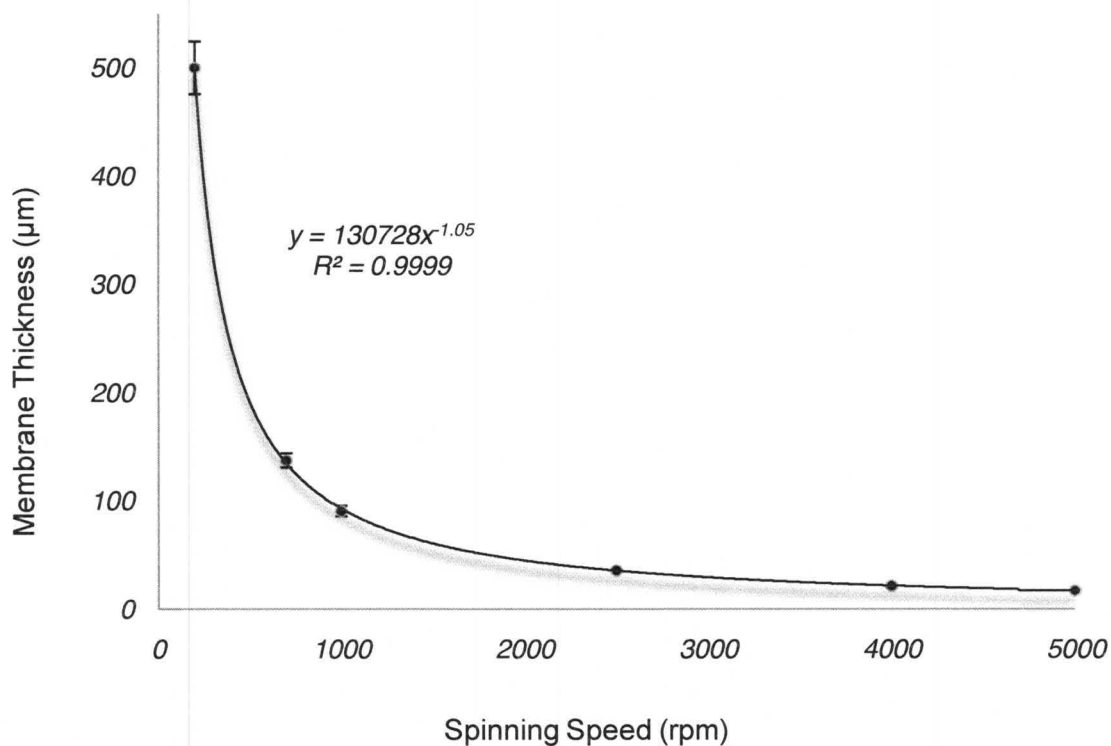
Figure 3.3. Membrane thickness versus spinning speed. The membrane thickness as a function of spin speed can be estimated using the equation y= `130728 $x^{-1.05}$.

3.5.3. Cell culture chamber and medium reservoir

To make a cell culture chamber with a thickness of 0.35 cm, a 65 g of the degassed PDMS mixture (10:1 ratio, as in the session 3.2 above) was molded evenly in a 15 cm diameter Petri dish and cured completely at 75 °C in an oven (Fisher Isotemp, Florence, KY) for at least 3 h. Then, the molded PDMS was removed from the Petri dish and a

rectangular piece of PDMS (7.5 cm x 3.0 cm x 0.35 cm) was cut. A hole (d= 1.4 cm) was

punched at the center of this PDMS rectangular piece using a cork borer #7 (CB #7)

(Fig. 3.4). A horizontal channel was created from the center to the outside edge of the

PDMS rectangular piece with the use of an 18 gauge (18G) blunt syringe needle

(SmallParts, NE181PL-C). The PDMS piece was then cleaned with the clear adhesive

tape to remove the dust particles from the surface.
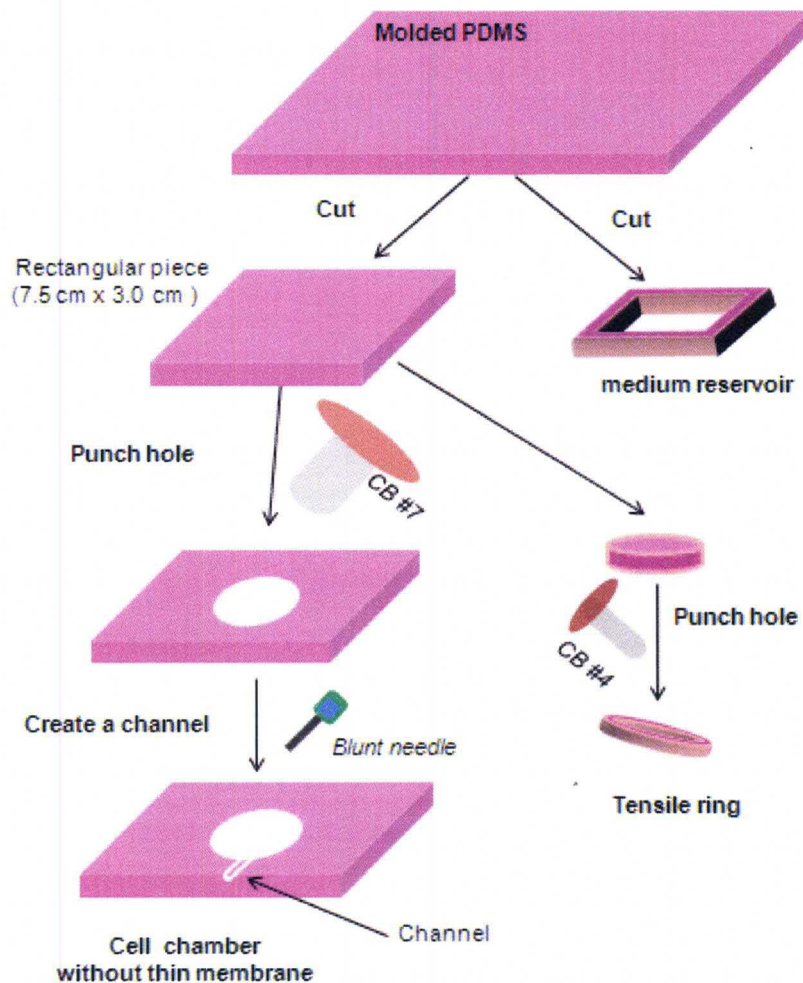
Figure 3.4. Schematic representation of fabrication steps involved in construction of the cell

chamber, the tensile ring, and the medium reservoir.

The PDMS piece and the thin PDMS layer were bonded irreversibly following exposure to O_2 plasma in a reactive ion etcher (RIE March Instruments) with 10% oxygen plasma, 100 mmTorr, and 100 mmHg. After a 30 second exposure, the pieces were aligned and bonded and subject to heating for a period of 10 minutes at 115 ^{o}C on the 110^0 hotplate to enhance the quality of bonding. Finally, the PDMS rectangular piece with the thin membrane at the bottom was gently peeled off from the silicon wafer to form a cell culture chamber (Fig. 3.5).
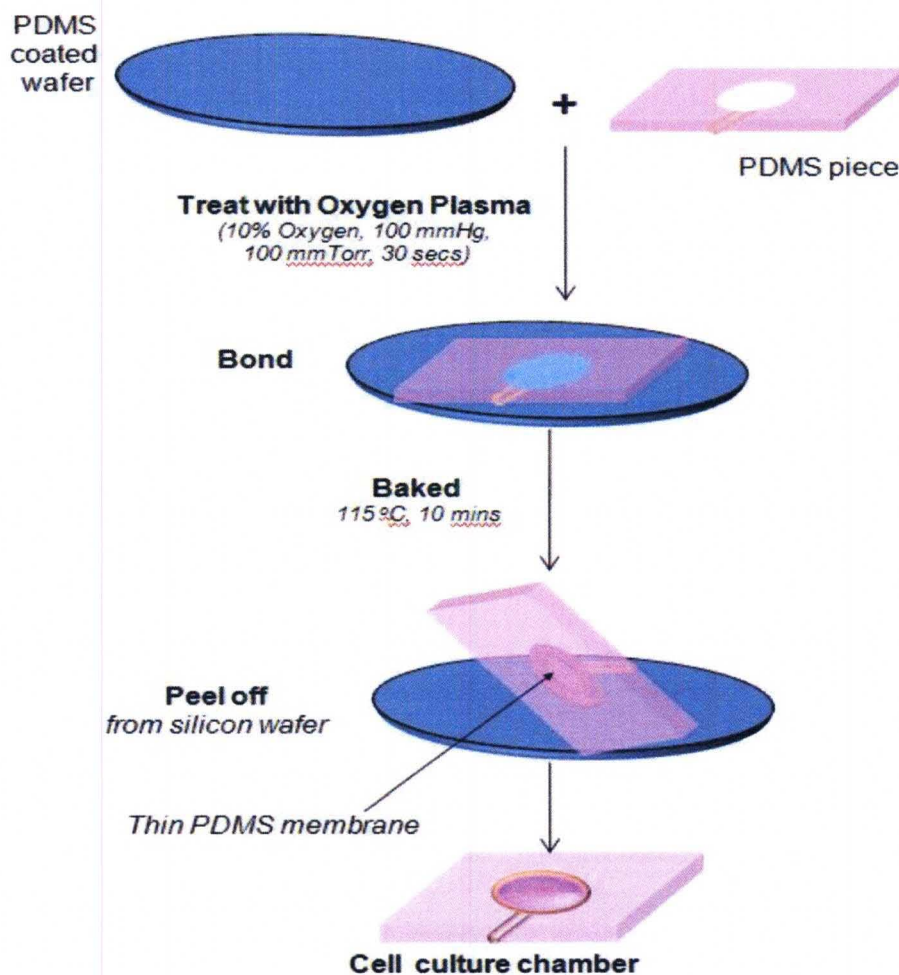
Figure 3.5. Procedure for fabrication of cell culture chamber

33

To make a tensile ring (0.8 cm inner diameter, ID, and 1.4 cm outer diameter, OD), the 1.4 cm diameter piece removed from the center of the rectangular piece made above was punched again at the center with a CB #4 (Fig. 3.4). To provide enough medium for the cell culture, a medium reservoir was also made of PDMS. A hollow PDMS rectangular piece (4.0 cm x 3.0 cm outside and 3.0 cm x 2.0 cm inside edges) was cut from the PDMS in a Petri dish (Fig.3.4). Clear adhesive tape was used to remove the dust particles from the reservoir and the tensile ring.

3.5.4. Oil chamber

To make the oil chamber, a rectangular PDMS (7.0 cm x 2.5 cm x 0.35 cm) was cut and a hole (d= 1.7 cm) was punched at the center with the use of a CB #9. An 18G blunt syringe needle was used to create two horizontal channels on either side and two 16G blunt syringe needles were inserted into these channels. This rectangular PDMS piece with the needles was placed on an acrylic sheet (7.0 cm x 2.5 cm x 0.25 cm) (Fig.3.6). PDMS was used to glue the holed PDMS rectangular piece with the acrylic sheet. An acrylic flat surface post (d= 0.85 cm, h =0.35 cm) was placed at the center of the hole of the PDMS rectangular piece and glued with PDMS. The pieces were placed in an incubator at 75 °C for 10 min.

3.5.5. Collapsible valve

The collapsible valve was assembled by inserting two ends of a 6 cm long Latex Penrose tube (ID = 5 mm, OD = 5.5 mm, ARGYLE™ Penrose Tubing) into 2 Teflon tube (OD= 0.65 cm, l=10 cm) (Fig. 3.7.). Then, this setup was inserted inside of a Poly Alloy™ T-

connector (¾ x ¾ x ½ inches, ApolloPEX). The ends of the T-connector were sealed tightly with PDMS rings (3 for each end, h = 0.35 cm, ID = 0.7 cm, OD = 1.95 cm). These PDMS rings ensured that no air leaked out of the T-connector when air was pumped from the pressure generator.
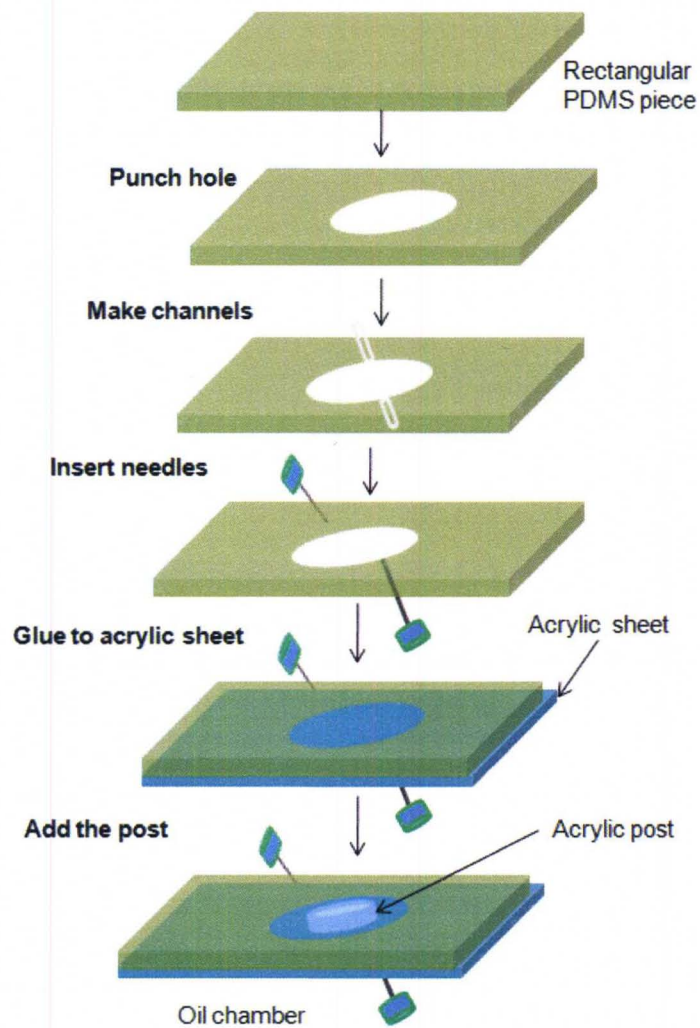
Figure 3.6. Fabrication and assembly of the oil chamber.
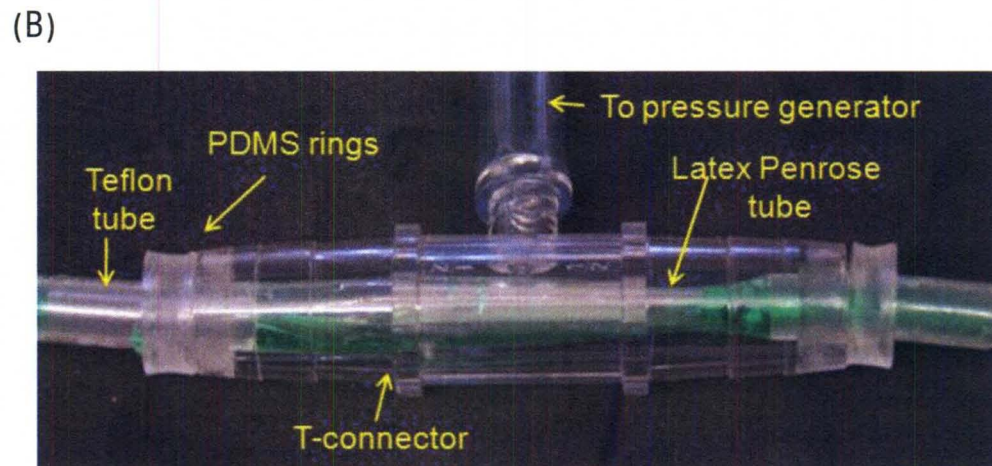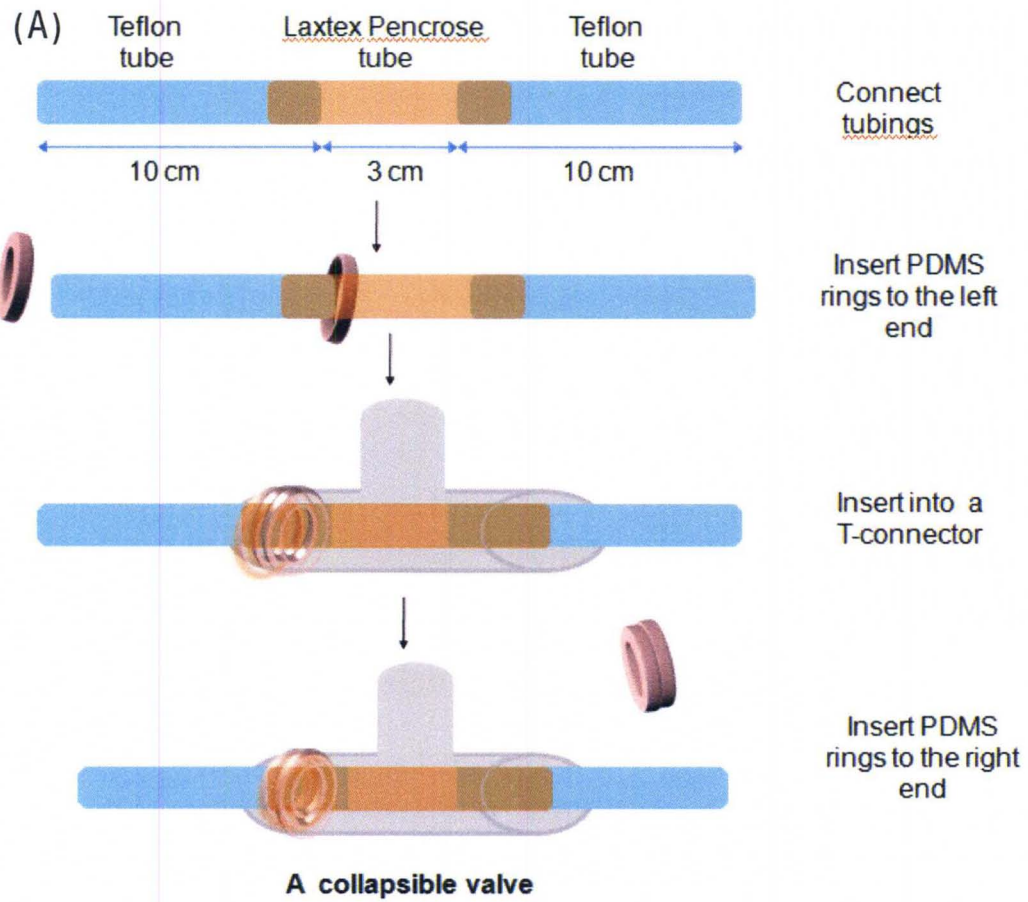
Figure 3.7. Assembly of the collapsible valve. (A) Steps to assembly the collapsible valve and (B) Assembled collapsible valve.

3. 6. ASSEMBLY OF THE µCCCM

To establish supporting base for the oil chamber, an acrylic sheet (7.0 cm x 2.5 cm x 0.25 cm) was placed in the rectangular hole on the bottom piece of the platform followed by the oil chamber (Fig. 3.8). Then, the cell culture chamber, with 18G needle inserted, was aligned on the top of the oil chamber in such a way that the post was centrically underneath of the thin PDMS membrane. The top piece of the platform was laid on the top of the cell chamber. The platforms were tightened with four screws. Finally, low viscosity oil was injected into the oil chamber through needles.
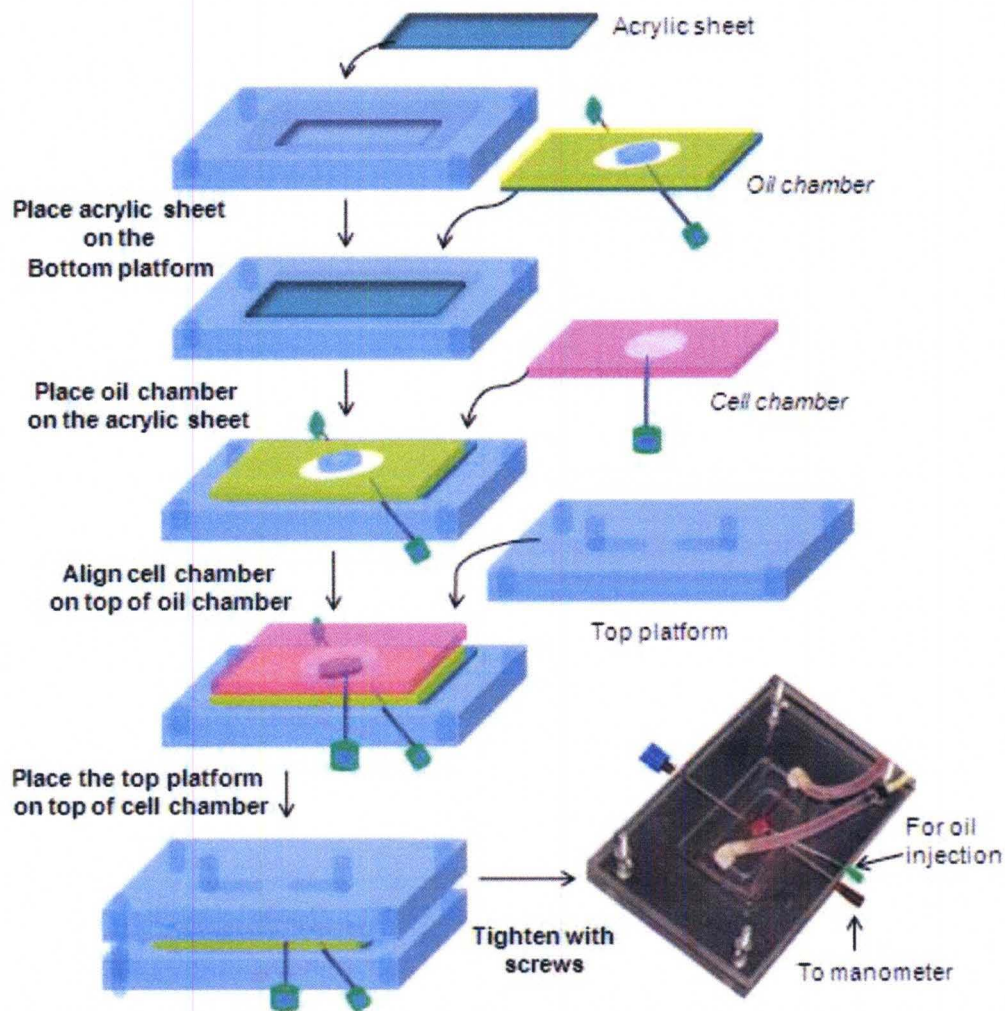
Figure 3.8. Assembly of the cell culture and oil chambers between the platform.

A 3-stop Pharmed BPT tube (1.3 mm ID, Cole-Parmer, Vernon Hills, IL) was connected from a 50 mL medium container to the inlet of the device via a peristaltic pump (Ismatex, ISM 596D, Vancourver, MA). The collapsible valve was connected from the outlet of the device to the medium container. The tunable valve was placed downstream of the collapsible valve (Fig.3.9). Finally, the pressure sensor was connected to the needle which was connected to the cell chamber. A pulsatile pressure generator was connected to the bottom T of the collapsible valve.
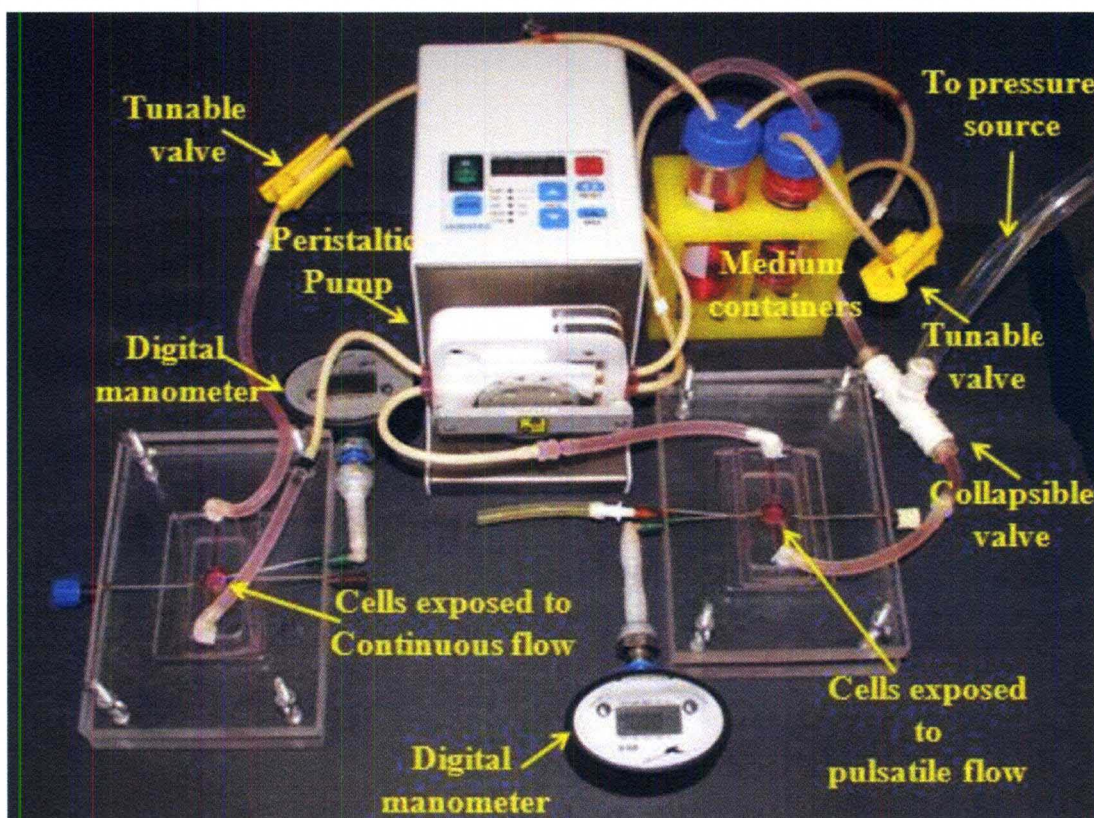
Figure 3.9. Assembled μCCCM for cell culture experiment. In this picture, two cell culture system were set up: the system on the left side was for flow only without valves (control). The other system on the right side has a tunable valve and a collapsible valve. Both systems have a circulating fluid network.

3.7. OPERATION OF THE μCCCM

Once assembled as in Fig. 3.9, the pump was started with an initial flow rate of 3.0 mL/min for about 30 minutes to enable seeded cells to gradually adapt device conditions. After 30 minutes, the flowrate was gradually increased until it reached 8.6 mL/min and the system was run for extra 15 more minutes. Then, the pressure in the pneumatic pressure generator source was gradually increased and tunable valve adjusted until the pressure reached the desirable values. The pressure was increased about 15mmHg every 15 minutes (refer to Appendix E for further detail information about the operation of μCCCM). Variable parameters such as the frequency of the membrane stretching as well as the percentage of systolic phase per one cycle were determined based on the requirement of each experiment. The frequency of the stretching was controlled through the % systolic and the frequency control on the pressure generator source. The pressure inside the cell chamber was varied by the corroboration between the pressure applied on the collapsible valve and the adjustment of the tunable valve. The stretching level of the membrane was determined by the thickness of the membrane and the pressure applied on the membrane. And the shear stress on the cells is controlled by the velocity of the fluid loading and the dimension of the cell culture chamber. For proof of concept studies, peak pressures of 120 mm of Hg, strain of 20% and a frequency of 80 bpm with 50% systolic to diastolic were used.

3.8. CONCLUSION

The μCCCM were created based on the mechanical loading conditions observed in the heart and a combination of techniques for mechanical stimulation on cells *in- vitro* cells.

When working with different types of cardiac cells, it is important to ensure that the type of mechanical loads delivered such as the stress, stretching, frequency of stretching, and the shear stress can be dynamically controlled. The μCCCM allows for dynamic studies, accomplished via direct manipulation of flow rate, valve operation, membrane thickness and the height of the cell culture chamber. This system is capable of accurately mimicking preload and afterload experienced in the healthy and failing heart.

CHAPTER IV- CHARACTERIZATION OF PRESSURE, STRETCH, AND SHEAR STRESS

4.1. INTRODUCITON

Application of the μCCCM for *in-vitro* studies of CVDs requires establishment of the ability of the system to simulate mechanical loading conditions associated with cardiovascular diseases observed *in-vivo*. These include the differences in pressure inside the chamber, strain that the cells experienced during the stretching, and the shear stress that the cells are exposed, specifically for cardiac endothelial cells. Pressure inside a left ventricle is an important factor that determines the contractility and the relaxation of the cells; therefore, different conditions associated with normal, high and low pressure such as heart failure, hypertension and hypotension were simulated using this system. In addition, the frequency of the heart beat was also varied to mimic conditions such as bradycardia and tachycardia. The percentage of the strain often varies in response to changes in preload and afterload seen in various manifestations of CVD. Other parameters associated with cardiac tissue like stretch and shear stress have also been accurately replicated. This chapter details all experiments performed to characterize the system.

4.2. PRESSURE CHARACTERIZATION

4.2.1. Setup of the µCCCM system

The device was assembled and the pressure build-up within the chamber was characterized for the following clinically relevant experimental conditions – (1) normal, (2) heart failure, (3) hypertension, (4) hypotension, (5) tachycardia, and (6) bradycardia. To accomplish pressure monitoring within the chamber, a small hole was punched using a 24 gauge syringe needle. An 18 gauge needle was then inserted into the hole to form a tight seal and attached to a hemostatic valve using luer connectors. A high-fidelity pressure catheter (Millar Instruments, Boston, MA) was inserted through a hemostatic valve and syringe needle such that the pressure sensing element resided in the center of the chamber. The chamber pressure data were signal conditioned and analog-to-digitally converted at a sampling rate of 400 Hz in 30-second recording epochs and stored for digital analysis with a clinically approved Good Laboratory Practice – compliant data acquisition system. The transducers were pre- and post-calibrated against known standards to ensure measurement accuracy. The chamber pressure waveforms were analyzed by using a Hemodynamic Evaluation and Assessment Research Tool program developed in Matlab (MathWorks, Natick, Mass).

4.2.2. Results

For various simulated conditions in the setup shown in Figure 4.1, the pressures inside the chamber were monitored and recorded. For a rate of 75 bpm, and a 40% systolic fraction, the µCCCM produced a peak pressure of 123 mmHg and an end diastolic pressure of 10 mmHg. The simulation of heart failure showed a lower peak pressure of

95 mmHg and a higher end diastolic pressure of 27 mmHg. Both hyper- and hypotension test simulation produced normal end diastolic pressures (8-10 mmHg). Simulation of hypertension resulted in a peak pressure of 183 mmHg while peak pressure
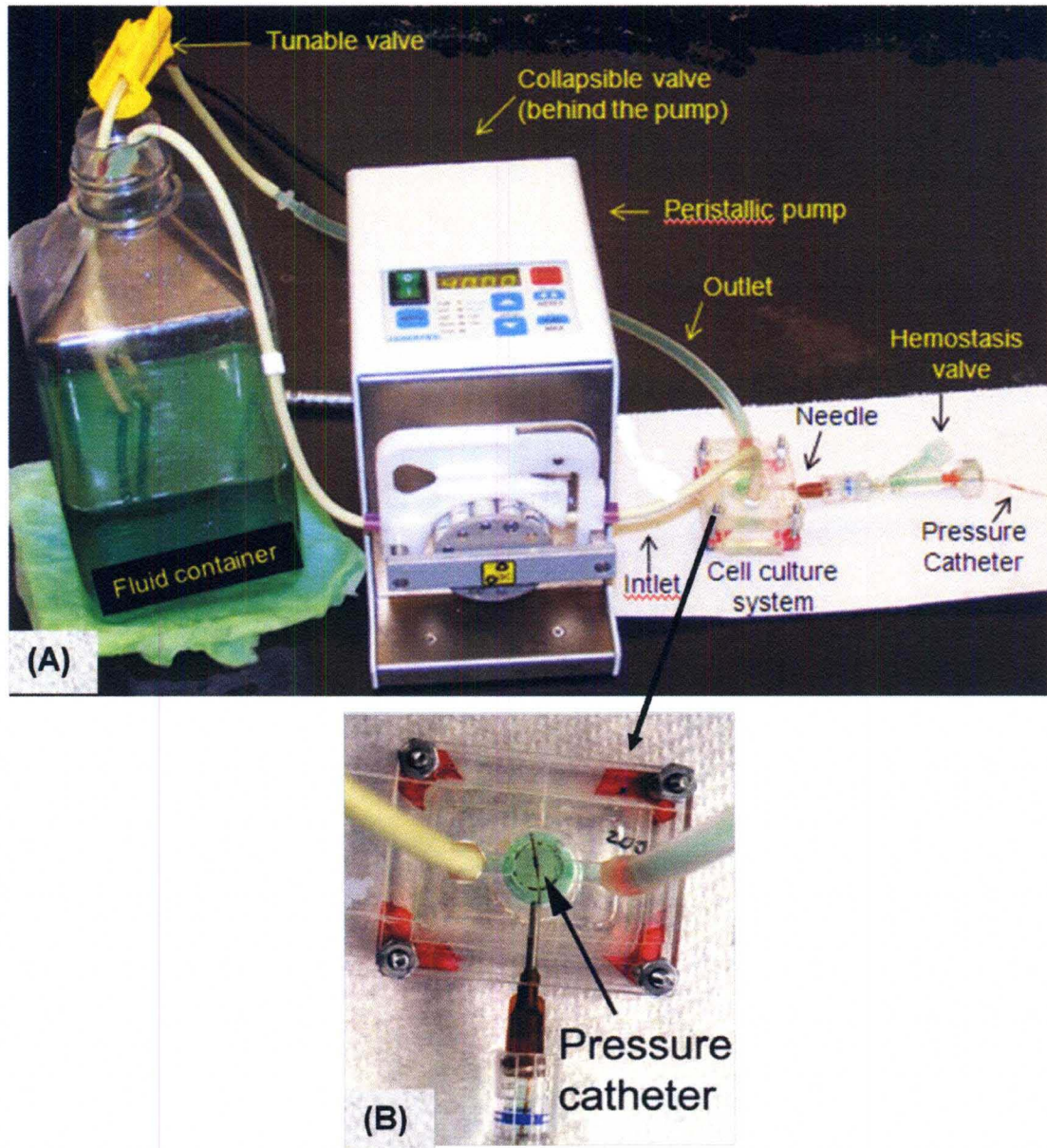
Figure 4.1. Setup for pressure characterization. (A) The whole setup; (B) Pressure catheter inserted into the cell chamber.

(92 mmHg) was achieved for hypertension. Tachycardia simulations resulted in a significantly higher beat rate (>200 bpm), lower end diastolic value (3 mmHg), and a higher systolic fraction (55%) compared to normal test condition. Simulated bradycardia showed a lower beat rate (46 bpm), and slightly lower systolic fraction (38%) compared to normal test condition. The values and waveforms obtained with the use of the μCCCM (Table 4.1 and Fig. 4.2) closely match those found in the literature for human left ventricular.

4.2.3. Discussion

As shown in Figure. 4.2, the peak pressures of the waveform obtained in the μCCCM system could be considered as end systolic pressure and the lowest peak as end diastolic pressure. The patterns of these waveforms could be explained through the concept of heart loading mentioned in the session 1.4. When the collapsible valve was closed, fluid accumulated inside the chamber in similar fashion to preloading in the heart. The pressure buildup in the closed chamber resulted in stretching of the membrane. This mimics the isovolumetric contraction of the heart. Once the membrane began to stretch, the volume of the chamber increased and the pressure inside the chamber also increased but slowly. When the collapsible valve was opened, fluid inside the chamber was released, causing the pressure to decrease. Initially, the reduction of the pressure was not significant due to energy recovery of the membrane and the fluidic resistance caused by a tunable valve. However, once the membrane was fully restored, isovolumetric relaxation occurred and the pressure decreased significantly, back to the initial pressure. This process mimics the diastolic phase and the afterload condition in the heart.

Table 4.1. Different parameters corresponding to mechanical loading of the left ventricle were replicated using the μCCCM. These parameters include heart rate, systolic fraction, end systolic pressure, and end diastolic pressure. LVP (left ventricle pressure).

Condition	Heart Rate (bpm)	Systolic Fraction (%)	LVP systolic pressure (mmHg)	LVP end diastolic pressure (mmHg)
Normal	75	40	123	10
Heart Failure	75	40	95	27
Hypertension	75	40	183	8
Hypotension	75	40	92	11
Tachycardia	200	55	112	3
Bradycardia	46	38	115	10

In HF, the end-systolic pressure is lower but the end-diastolic pressure is higher than normal heart condition. This condition was reproduced by the μCCCM. This was obtained by reducing the pressure of the pressure generator source (the collapsible valve not fully collapsed) and increasing the fluid resistance through the tunable valve.

Cardiac hypertrophy and hypotrophy conditions occur when the pressure inside the heart is high or low respectively but the contractile function of the cells is still normal to eject all the blood into the body. As a result, the end systolic pressure is either high
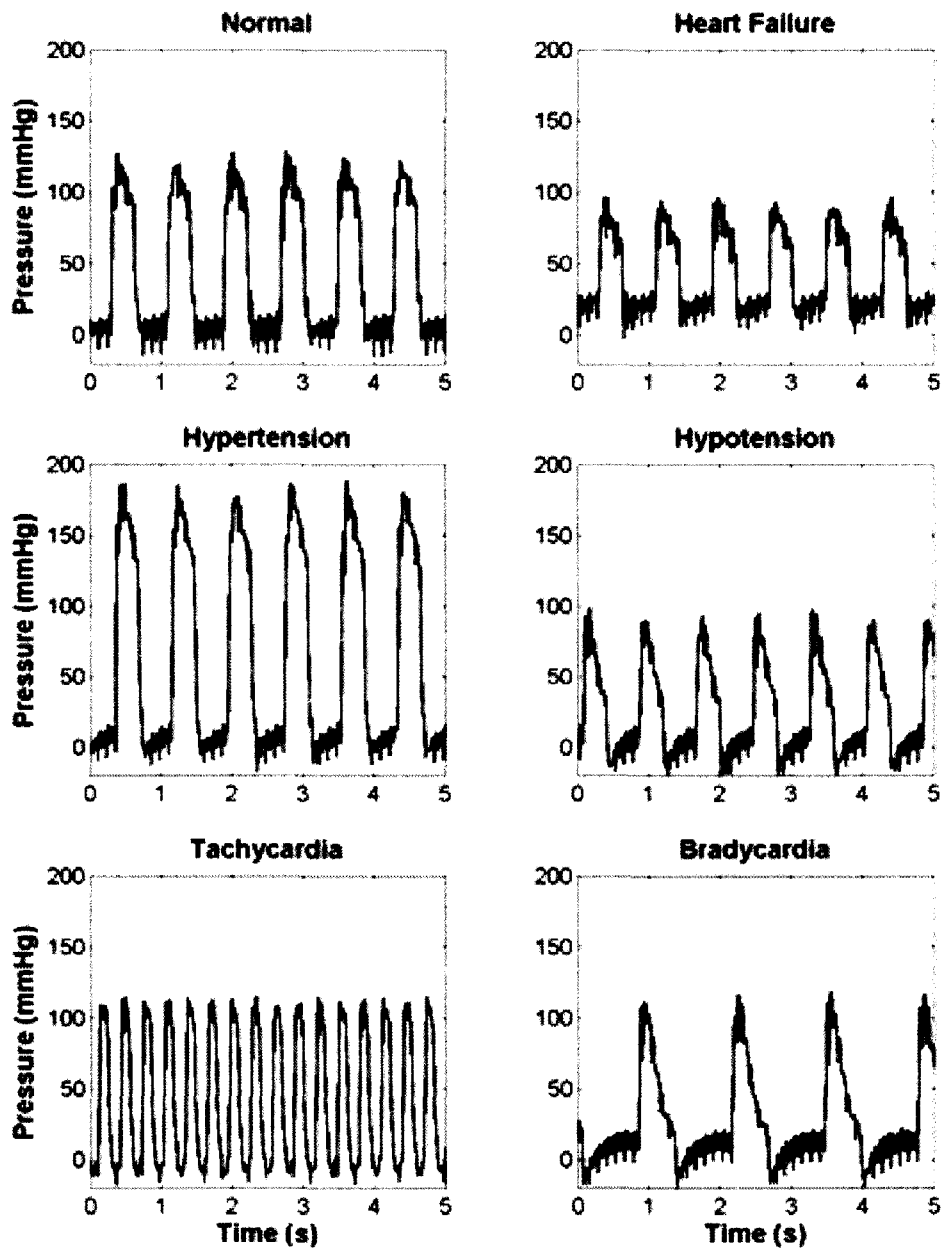
Figure 4.2. Pressure waveforms for various physiologic conditions replicated using the μCCCM. These conditions include both normal and dysfunctional myocardium, such as, heart failure, hypertension, hypotension, bradycardia, and tarchycardia. These results confirmed that the μCCCM enabled to recreate various clinically relevant physiologic conditions.

(hypertension) or low (hypotension) while the end diastolic pressure is the same as in normal heart condition. These conditions were also recreated under the μCCCM system by either increasing or decreasing the pressure in the pressure generator in order to control the closure level of the collapsible valve and by adjusting the tunable valve. Lower or faster frequency of the heart beating can create health problem. Tachycardia condition occurs when the heart beat is between 150 bpm to 200 bpm.[56]. In contrast, the heart beat in bradycardia condition is lower than 60bpm.[50] To eject all the blood out of the heart, the systolic fraction under tachycardia condition needs to be increased, but this fraction needs to be decreased in bradycardia. In addition to the beat frequency, both the end-systolic pressure and end-diastolic pressure must be the same as in normal condition. These conditions were obtained in the μCCCM by increasing or decreasing the systolic fraction per cycle and the frequency of the heart beat in the pressure generator.

In conclusion, the manipulation of different elements of the μCCCM enabled recreation of various clinically relevant physiologic conditions of the heart.

4.3. STRAIN CHARACTERIZATION

4.3.1. Setup of the μCCCM system

Strain developed on the thin membrane was experimentally evaluated. Before assembling the device, the post surface and the outside bottom of the thin membrane were marked with tinny black dots by a fine marker (Fig.4.3A). Then, the cell chamber and the oil chamber were assembled as explained previously (sessions 3.5 & 3.6). For

the strain characterization, a 30 mL syringe filled with water and a hemostatic valve were connected to the inlet and outlet of the cell chamber, respectively. The syringe was used to apply different pressures to the cell chamber via fluid loading (Fig.4.3B). To measure the pressure inside the chamber, a digital manometer dV-2 was used. To track the position and displacement of the dots, a CCD camera coupled to fluorescence microscope (Nikon Eclipse TE2000-U) was used.
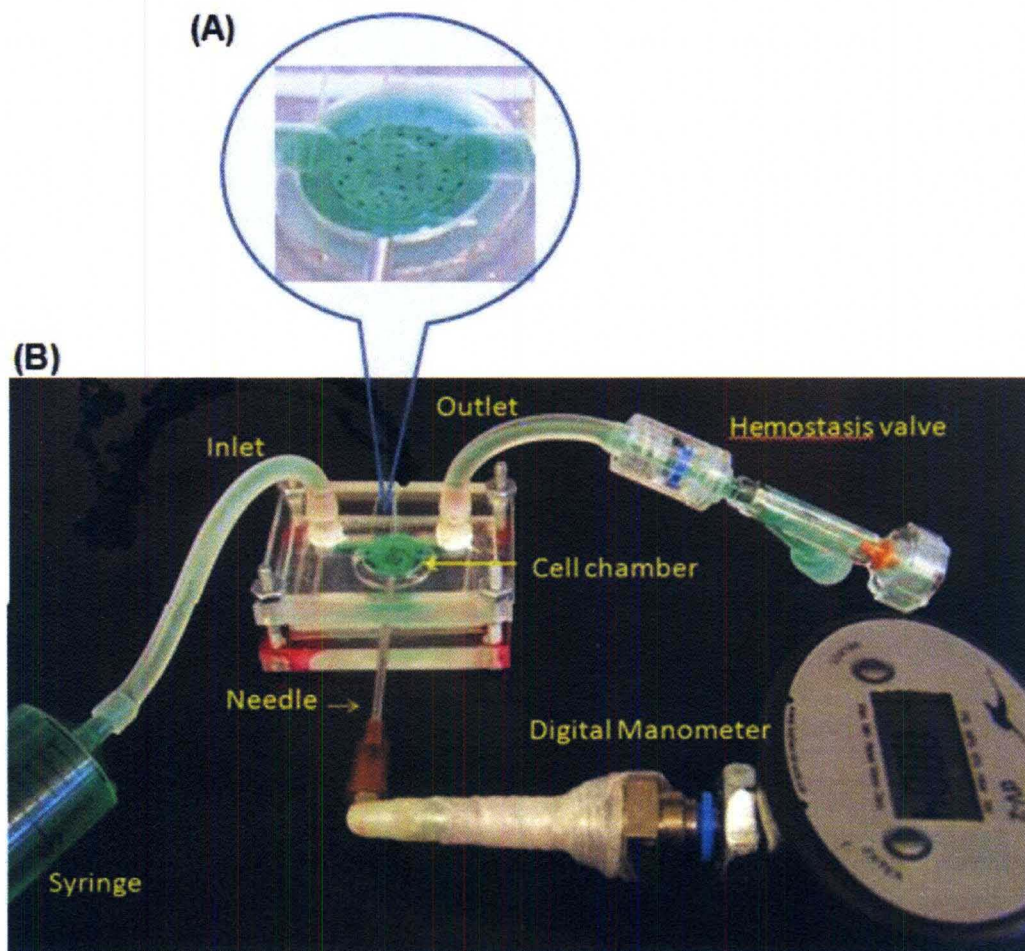
Figure 4.3. Setup for strain characterization. (A) Membrane and the post marked with black dots, and (B) Entire setup for the strain characterization.

4.3.2. Operation of the system

Water was injected slowly with the use of the syringe into the cell chamber. After the chamber was totally filled with water, the air bubbles trapped in the cell chamber were removed. Then, the hemostatic valve connected to the outlet was closed. To increase or decrease the pressure inside the chamber, the syringe was gently pushed or pulled. The baseline pressure was set up as 0.0 mmHg.

Under the microscope, the dots on the post were considered as the reference points while the dots on the membrane were tracked with a CCD camera while pressure was applied. To measure the strain, pictures of the membrane were taken before and after the application of the pressure. Then, the distance between the reference point on the post and a dot on the membrane were measured before (L_0) and after (L_f) the application of the pressure. The data was then analyzed using Microsoft Excel.

4.3.3. Results

Five different membrane thicknesses were used (329 μm, 192 μm, 135 μm, 93 μm, and 35 μm) and five different pressure values (60 mmHg, 80 mmHg, 100 mmHg, 120 mmHg, and 140 mmHg) were applied to each membrane. At least five different changes of relative positions were measured for each experiment. The % strain values and standard deviation for different pressures and membranes were calculated.

$$\% Strain = \frac{(L_f - L_0)}{L_0} 100$$

where, L_0 is the length between two dots at 0.0 mmHg and L_f is the length after pressure was applied.

The pressure and the percentage strain values as a function of the pressure applied for each membrane are shown in Table 4.2 and Figure. 4.4. As can be seen from Figure 4.4, the strain values correlate linearly with the pressure applied on the membrane. Moreover, the percentage of the strain increases when the thickness of the membrane decreases. By varying the thickness of the membrane and the pressure applied on the membrane, the percentage strain obtained could be as low as 4.15% and as high as 60.2%. The % strain of the cells in the heart is anywhere between 5% to 25%.[57], [58]

Table 4.2. % strain determined for various pressures on membranes with different thicknesses.

Pressure/thickness	329 µm	192 µm	135 µm	93 µm	35 µm
(mmHg)	strain (%)	strain (%)	strain (%)	strain (%)	strain (%)
60	4.158	5.242	15.189	27.313	18.280
80	4.884	6.632	18.659	36.535	26.711
100	6.450	10.203	21.740	48.778	34.363
120	7.788	11.665	23.614	54.884	40.369
140	8.257	14.617	26.932	62.260	42.358

The error bars in the Fig. 4.4 are large due to two main reasons. First, the pressure sensor has a low frequency that is not sensitive to the precise pressure changes in the cell culture chamber. Second, the post underneath of the membrane was not aligned exactly at the center of the membrane, causing the variation of the membrane stretching on the post.

50
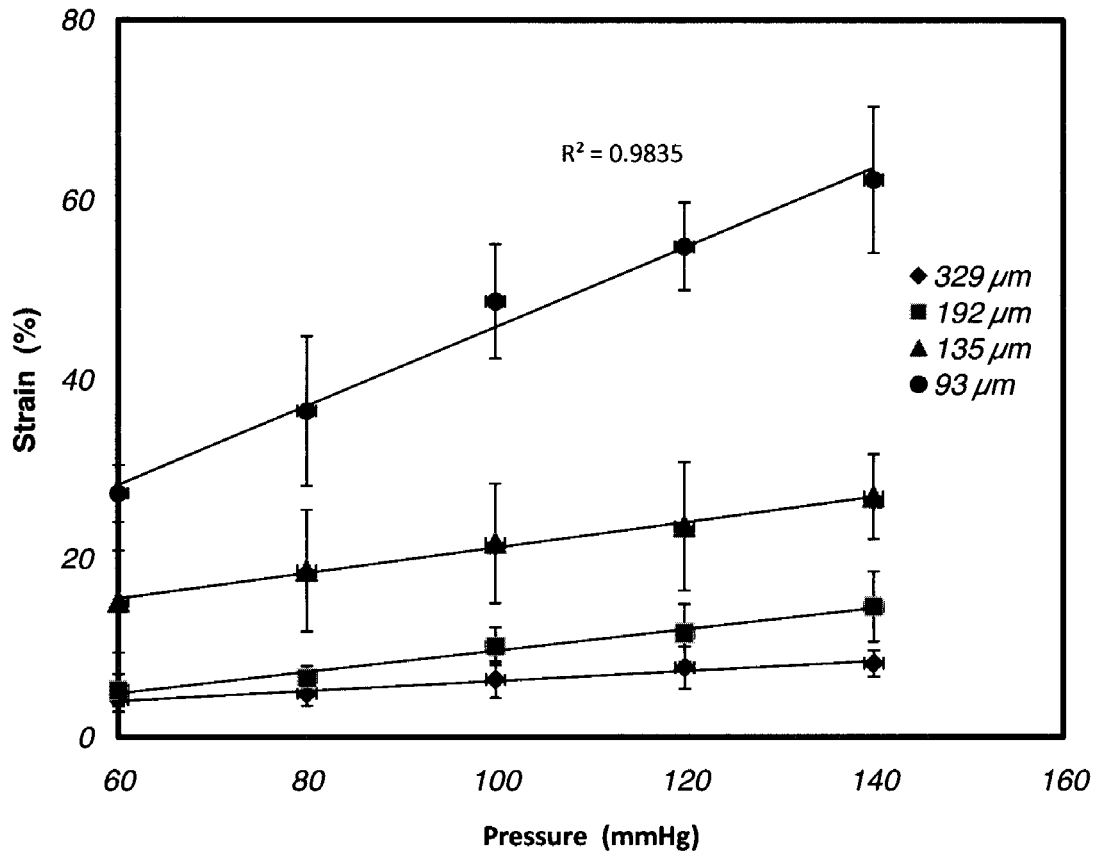
Figure 4.4. % strain as a function of pressure for different membrane thicknesses.

4.3.4. Discussion

In addition to the pressure stimulation, stretch levels in cardiac cells play a critical role ensuring cell phenotype and function. In the μCCCM system, cardiac cells were attached and grown on the thin PDMS membrane and the % strain of the PDMS membrane represents the stretch level of the cells growing on it. The result showed that the % strain of the membrane was determined by the thickness of the membrane and the loading pressure. The % strain was directly proportional to the pressure but inversely proportional to the thickness of the membrane.

In conclusion, base on the % strain found for the PDMS membranes and the % strain that the cells are exposed in the heart, these membranes could replicate in vivo stretch experienced in the heart.

4.4. SHEAR STRESS MODELING

4.4.1. Method

Finite element software ANSYS Academic Teaching Advanced 12.0, FLOTRON module, was used to generate the wall shears stress as a function of channel height and flow rate. The system modeled using a 2D simulation and environment was verified for steady incompressible flows. For the simulation, it was assumed that the participating fluid has the same physical properties of water, including the density (ρ = 1000 kg m-3) and dynamic viscosity (μ = 10 Pa s). The inlet fluid flow rates of 8.6 mL /min, was applied while the outlet was set as zero pressure. It was also assumed no-slip boundary conditions for the channel and groove walls. The fluid domain was meshed using 2D quadrilateral element, FLUID141, to model steady state fluid. A segregated sequential solver algorithm was used; that is, the matrix system derived from the finite element discretization of the governing equation for each degree of freedom was solved separately. The mesh was refined through mesh sensitivity analyses: at each simulation, the elements showing high velocity gradients were refined, until reaching convergence of sensitive measures of the predicted quantities.

4.4.2. Results

Four wells with different depth (0.25, 2.00, 4.00, and 8.00 mm) were used; and a velocity of ~ 0.024 m/s at the inlet of the wells was applied in all the experiments. The shear stress (τ) was determined using the equation [59]

$$\frac{du}{dy}$$

where τ is the shear stress(dynes/cm^2), μ is viscosity coefficient (kg/(m.s)), u is the fluid velocity (m/s), and y is the thickness of the well (m). The viscosity (μ) of water at 1atm and 20 $^{\circ}$C is 1.0 x 10-^{3} kg /(m.s).[59]

4.4.3. Discussion

The shear stress simulation (Fig. 4.5) showed that for the wells with depth of 2.00, 4.00, and 8.00 mm, the shear stress was nearly 0.0 dynes/cm^2 at the bottom of the well to approximately 200 μm above of it. However, for the well with a 0.25 mm depth, shear stress was significantly high (~ 10 dynes/cm^2) at 200 μm from the wall and below, in the region where cells were cultured within the device. An additional variable which has a major effect on shear stress but was not evaluated due to cascading effects on pressure and stretch is the inlet fluid flow velocity. This characterization affirmed that the μCCCM can monitor the shear stress based on the height of the cell chamber and the velocity of the fluid flow.

(a) Well Depth: 0.25 mm

(b) Well Depth: 2 mm

(c) Well Depth: 4 mm

(d) Well Depth: 8 mm

| 0 | .003957 | .007913 | .01187 | .015827 | .019783 | .02374 | .027697 | .031653 | .03561 |
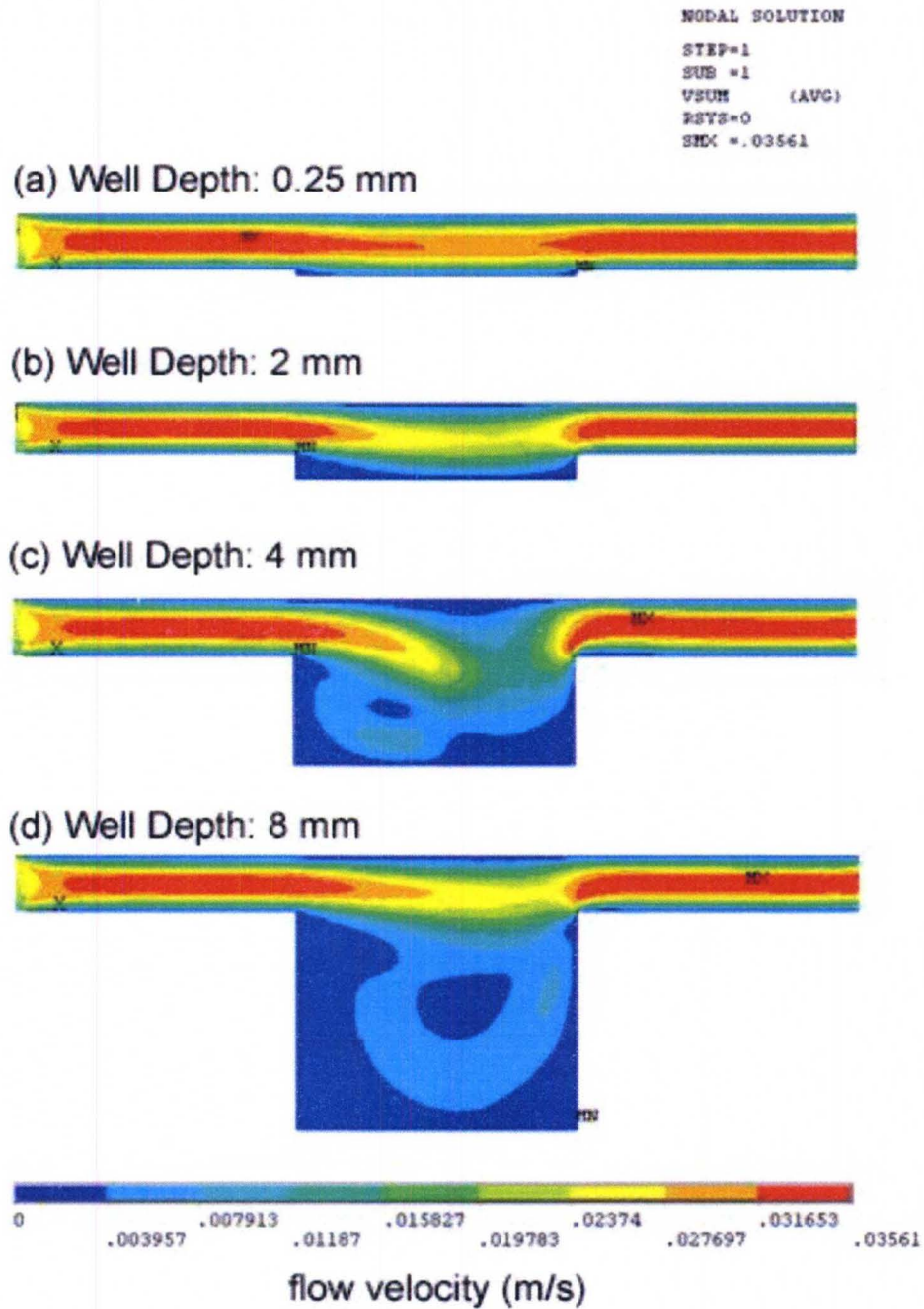
flow velocity (m/s)

Figure 4.5. Shear stress simulation for the cell culture chamber of the μCCCM. This shear stress was simulated with an inlet flow velocity of 0.024 m/s and various well depths.   Note that the shear stress is negligible in the region where cells are cultured for all well depths except the 0.25 mm deep well.

54

4.5. CONCLUSION

Overall, the characterization of pressure, strain, and shear stress affirmed strongly that the μCCCM can be used to replicate the *in-vivo* heart function. This replication can be accomplished through a combination of different variables such as membrane thickness, the height of the cell chamber and adjustment of tunable components including the collapsible valve, tunable valve, the peristaltic pump, and the pressure generator.

CHAPTER V- CELL CULTURE WITHIN THE μCCCM

5.1. CELL CULTURE WITHIN THE μCCCM

Cardiac tissue is 3-dimensional and consists of cells within an organized extracellular matrix. Cells cultured *in-vitro* are often grown in mono layers on tissue culture dishes or flasks. To demonstrate proof of concept of the ability of the μCCCM to establish cardiac cell culture *in-vitro*, H9c2 cells were cultured under normal mechanical loading conditions. Their ability to survive mechanical loading, phenotype, structure and function were evaluated using microscopy. Preliminary results indicate successful cell culture, establishment of an *in-vivo* like phenotype, alignment of f-actin stress fibers and increased activity representative of cardiomyocyte contractile function.

5.2. H9c2 CELL LINE

H9c2 is an immortalized cell line derived from embryonic BDIX rat cardiac tissue and has structural characteristics of a striated muscle cells.[60] An advantage of using this type of cell line as the first step for system validation is the fact that despite their unlimited lifespan, these cells still maintain their morphology, metabolic activities and gene expression. Therefore, the experiments can be repeated easily, and the results obtained are reproducible and reliable.

The characteristics of the H9c2 cells under mechanical stimulus are similar to those of striated muscle cells,[60], which are composed of sarcomeres as contractile units. When cultured in-vitro, H9c2 cells can attain different shapes depending on conditions for attachment and growth (Fig. 5.1). H9c2 can attain polygonal or flat spindle shapes, when they directly attached on the bottom of the culture dishes. Spindle shape cells usually arrange in parallel to one another. However, when the cells were on top of each other, they appear as spherical and angular shapes. In the quiescent culture condition, most cells are mono nucleated and most nuclei appear spherical and contain to several nucleoli.[60]
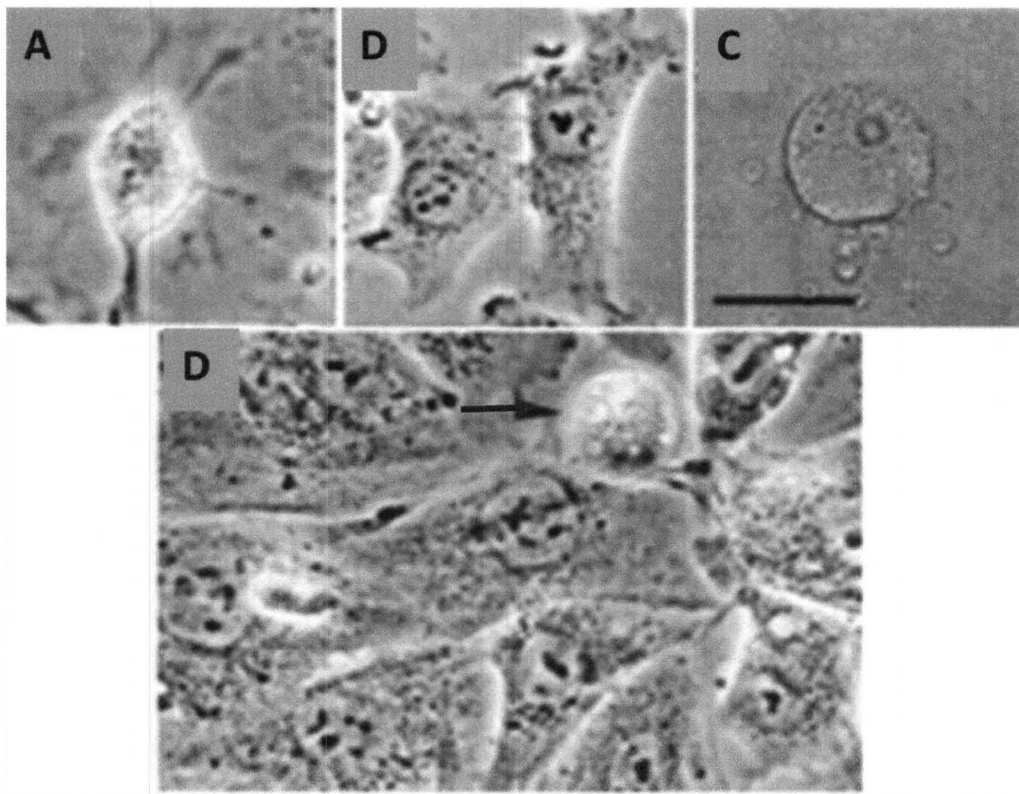
Figure 5.1. Different shapes of the H9c2 under the static condition: (A) An angular cell (B) Polygonal cells, (C) A spherical cell (D) A single spherical cell (arrow) on a densely grown layer.

5.3. CELL CULTURE

H9c2 embryonic cardiomyogenic cell line was used for all the experiments. The cells were maintained in culture using high glucose Dulbeco's Modified Eagles' Medium (Cellgro DMEM, 4.5 g /L glucose, Cat# 10-0130V, Herdon, VA) supplemented with 10% fetal bovin serum (Hyclone FBS, Cat # SV30014-03,Logan, UT) and 1% penicillin-streptomycin-glutamine (Cellgro, Cat # 30-009-CI, Herndon, VA). Detailed protocols and recipes are in the Appendix C and D.

5.3.1. Preparation of the cell chamber

For each experiment, three sets of cell chambers were needed: static culture condition, constant perfusion, and pulsatile stretch. The static and continuous flow sets were used as controls.

Two days prior to seeding, the thin PDMS membrane, tensile rings and medium reservoirs were sterilized with 70% isopropanol. The cell culture chambers with PDMS membrane (Session 3.5.3) was treated with 10% oxygen plasma for 1 min and then a sterilized 18G needle was inserted into the channel of the chamber (Fig 5.2). To accomplish patterning of cells, a tensile ring was then placed inside the well of the cell chamber to limit the cells to grow on a circular area of 0.8 cm diameter. A medium reservoir (Session 3.5.3) was added on the top of the chamber. The assembled cell culture chamber was filled with 100 µL of ECM solution (Appendix C.4). For sterilization, UV light was applied to the chambers for 4 min. Chambers with were incubated for 24 h at 37°C or for 3 days at 4 °C.
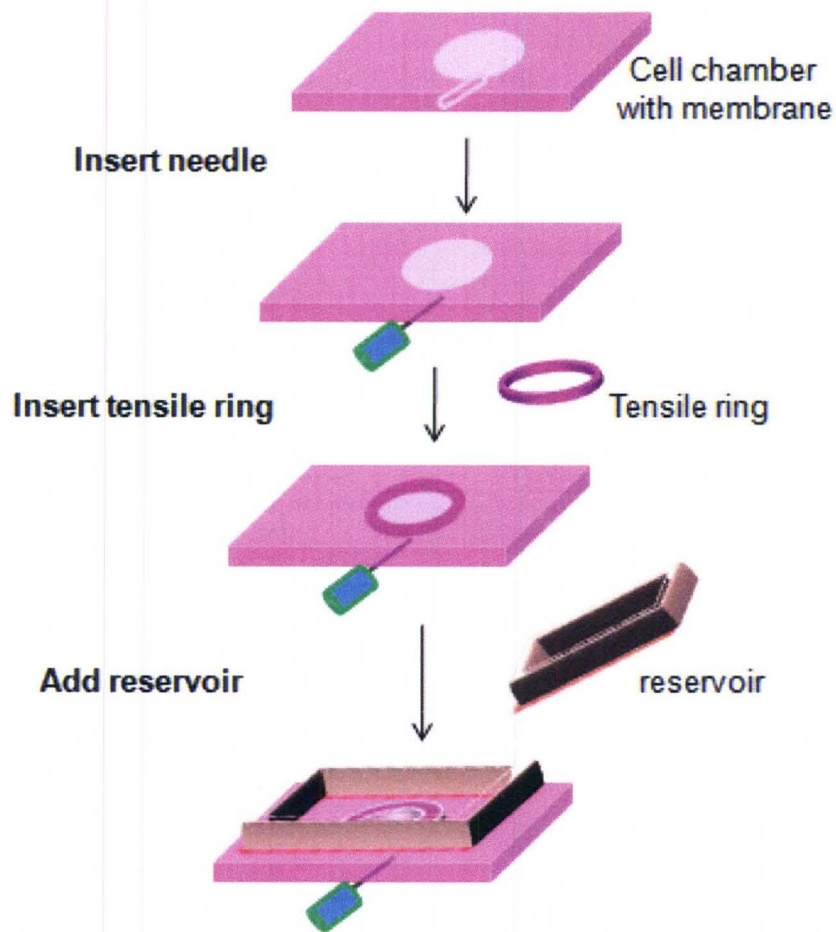
Figure 5.2. Assembly of the cell culture chamber. Insertion of the needle, addition of tensile ring, and medium reservoir.

5.3.2. Cells culture in the chamber

H9c2 cells in a cell culture flask were trypsinized, centrifuged and re-suspended in a fresh H9c2 cell culture medium. Before seeding the cells in the device, the ECM solution in the chamber was removed and the chamber was washed with warmed medium. Then, a 100 µL of resuspended cell solution (2.5×10^5 cells /mL) were added into the center of the well. The cells were allowed to attach and spread out for 4 h at 37 $^\circ$C. After 4 h,

approximately 1.0 to 1.5 mL warm fresh medium was added and the cells were incubated at 37°C for 48 h. Cell culture medium was changed every day.

5.3.3. Assembly of the µCCCM for cell culture

To avoid contamination, the assembly of the µCCCM was performed under the cell culture hood. After 48 h, cells in the chambers were 100% confluent. The medium reservoir and the tensile ring were gently removed and the outside bottom of the membrane where the cells were seeded was marked with tinny black dots by a fine maker. One chamber with the cells was used to culture the cells in static condition while the others two were used to culture the cells under constant perfusion (only flow) or under perfusion and pulsatile stretch (flow and pressure).

The cell culture devices were assembled as explained in Session 3.4. For constant perfusion, the collapsible valve was not used. Instead, only a Pharmed BPT tubing (1.3 mm ID, Cole-Parmer, Vernon Hills, IL) was connected from the outlet of the device back to the 50 mL medium container (Fig. 3.8). To check for leakage, the µCCCM was tested under the hood and then placed in the cell culture incubator to perform the experiments.

5.3.4. Operation of the µCCCM with cultured cells

Initially, cells were exposed to a flow rate of 2.0 mL /min for 15 minutes. Then, the flow rate was gradually increased to reach 8.6 mL /min. After 15 minutes, the pulsatile pressure was applied to the cell chamber and was increased slowly, from 15 mmHg /0

mmHg to 80 mmHg/0 mmHg, with 50% systolic and 80 bpm setup using the pressure generator. The pressure inside the chamber was monitored by a digital manometer dV-2 connected to the cell chamber.

After 24 h, the system was stopped gradually. First, the pressure was reduced slowly, then, followed by the reduction of the flow rate. The system was removed from the incubator and its parts were disassembled carefully. For immunofluorescence experiments, cells were fixed with warm 4% PFA immediately after the platforms were removed. Cells were immunostained or were placed at 4 °C.

5.3.5. Immunostaining

The fixed cells were immunostained for detection of phosphorylated-phospholamban (p-phospholamban) proteins and stained for visualization of f-actin. For detection of p-phospholamban, the primary and secondary antibodies were p-phosppholamban (Ser 16) (sc-12963, Santa Cruz Biotechnology, Santa Cruz, CA)) and FITC-conjugated chicken anti-goat (Alexa Fluor 488, Invitrogen, Carlsbad, CA) respectively. Both antibodies were diluted (1:100) in 1% BSA. The cells were incubated first with the primary antibody at room temperature for 1 h, followed by the addition of the secondary antibody for 1 h at room temperature. For f-Atin staining, TRITC-conjugated Phalloidin (1:100; Millipore, Billerica, MA) in 0.5% BSA solution was added to the cells and incubated for 1 h at room temperature. After the staining, light Diagnostics mounting fluid (5013, Millipore, Billerica, MA) was added. Phase contrast and fluorescent images were taken with the use of a CCD camera connected to a fluorescent microscope (20X, Nikon,

Eclipse TE 2000-U). MetaMorph Software Program was used for the analysis of the images.

5.4. EVALUATION OF CELLS USING MICROSCOPY

H9c2 cells were cultured in static condition (control) and within the μCCCM under pulsatile pressure and stretch, representing normal physiological loading. Cells cultured under flow only were not evaluated, but used just for the reference; therefore, it is not discussed in this session.

Cell cultured in static condition (control) attained a fibroblast like morphology (Fig. 5.3a) whereas cells cultured in the μCCCM were more rectangular, and presented a postage stamp-like morphology (Fig. 5.3b). The size of the cells cultured within the μCCCM exposed to pressure was larger than those cultures in static condition.

Staining with Phaloidin showed low intensity of the fluorescent color and random orientation of f-actin in controls in comparison to aligned f-actin in cells cultured with pulsatile pressure and stretch (Fig. 5.3c and d). This indicated that the contraction-stretching of the cells promotes the increasing % of f-actin and also an increase in the length of the sarcomere, and helps to align the cells in one direction. The increase in length of the sarcomere is the result of the increase in contraction of the cell under pulsatile stretch. The alignment of the cells demonstrated that mechanical loading spontaneously rearranged the orientation of the cells.

P-phospholamban was detected in cells cultured within the µCCCM, however the expression of this protein was very low in cells culture in static condition, as shown is Figure 5.3e, in comparison to the cells cultured in µCCCM (Figure 5.3f). Phospholamban is the integral membrane protein. To respond to the contraction of the cells, phospholamban is phosphorylated. With cAMP, this p-phospholamban promotes the influx of Ca^{2+} into the cells [61-62] to bind to the contractile unit, causing the cells to contract. Therefore, indirectly, the increasing of activation of p-phospholamban, which was reflected by the intensive green color on the loading sample in comparison of the color on the control sample on the Fig. 5.3e and f, will be indicative of cell contraction.

5.5. CONCLUSION

H9c2 cells were cultured within this device to demonstrate proof-of-concept of the ability of the µCCCM to sustain cell culture. The cells not only survived physiological loads in vitro but the effects of physiological loading were clearly evident when analyzed via microscopy. Cells within the µCCCM established an in-vivo postage stamp –like morphology, showed alignment of F-actin stress fibers and increased expression of p-phospholamban in comparison to static controls.
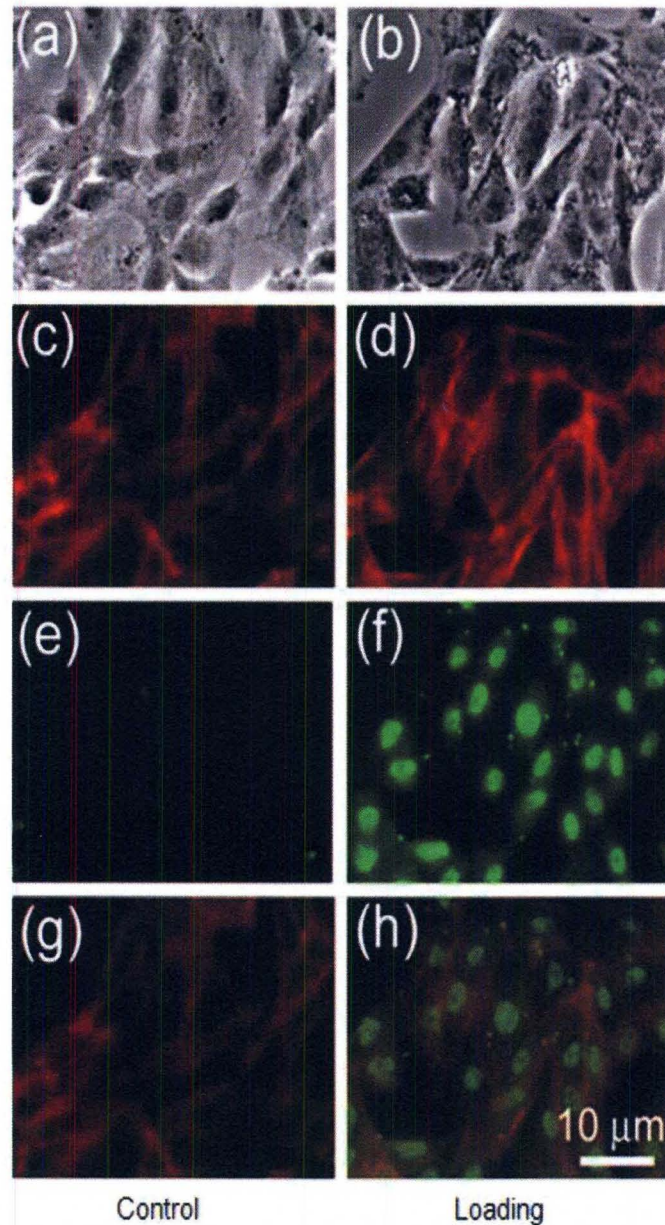
Figure 5.3. Physiological loading promoted the alignment of f-actin and increased phosphorylated phospholamban activity in H9cC2 cells. Cells were under static condition (control) and normal physiological loading for 24 hrs. Notice the directional alignment of f-actin stress fibers and increased p-phospholamban activity in the loading condition. (a, b) Phase contrast images; (c, d) Staining with TRITC-conjugated Phalloidin for detection of f-actin; (e, f) Immunofluorescence staining for detection of p-phospholamban activity; (g, h) Merged images of F-actin and p-phospholamban.

CHAPTER VI- CONCLUSION AND FUTURE DIRECTION

CVD continues to be a major healthcare problem worldwide. Current treatment options, though beneficial have significant limitations. In order to address these issues and provide new treatment options a better understanding of the molecular pathophysiology of CVDs is necessary. Cellular level models provide the best platform for discovery based studies. However, current approaches for cardiac cell culture fail to accurately replicate the mechanical loading conditions seen *in-vivo* as a consequence of normal hemodynamic loading and unloading. Available techniques address mechanical loading on an individual basis but to date, no system that accurately replicates the *in-vivo* mechanical loading environment exists. This has resulted in cell-level studies being conducted in environments with little or no physiological relevance.

The μCCCM was designed and developed to culture various cardiac cells in a physiologically relevant environment by replicating the mechanical loading conditions generated as a consequence of normal hemodynamic loading and unloading. Various variables like pressure, strain and shear can accurately replicated in a pulsatile fashion similar to conditions experienced in the heart. Characterization studies show that mechanical loading profiles associated with normal and various disease conditions of the heart including heart failure, hypertension, hypotension, bradycardia and tachycardia can be accurately replicated over extended periods of time. Finally, proof-of-concept studies

using H9c2 cells, a cardiomyocyte cell line confirms the ability of this system to culture cells within this platform and evaluation of cells using microscopy and immunofluorescence indicates establishment of an *in-vivo* like phenotype.

Thus far, characterization and proof-of-concept demonstrations were accomplished using this system. Confirmation of the ability of the µCCCM to accurately mimic the *in-vivo* cardiac environment allows for the design and study of various conditions associated with CVD. These studies include cardiomyocyte regeneration using mechanical loading and stem cells, adult cardiomyocyte regeneration using controlled mechanical loads, study of cardiac and aortic endothelial cells under conditions of continuous and pulsatile flow and finally evaluation of drugs and other treatment options using cardiac cells maintained under various disease conditions.

REFERENCES

1. *Cardiovascular Disease Statistics.* Available from: *http://www.americanheart.org/presenter.jhtml?identifier=4478.*

2. *Cardiovascular Disease Statistics.* 2010; Available from: *http://healthlibrary.brighamandwomens.org/RelatedItems/85,P00243.*

3. Murray, C.J.L., S.C. Kulkarni, and M. Ezzati, *Understanding the coronary heart disease versus total cardiovascular mortality paradox - A method to enhance the comparability of cardiovascular death statistics in the United States.* Circulation, 2006. **113**(17): p. 2071-2081.

4. *Cardiovascular Disease Types.* Available from: *http://heart-disease.emedtv.com/cardiovascular-disease/cardiovascular-disease-types.html.*

5. Lloyd, J., *Heart Disease and Stroke Statistics-2010 Update: A Report From the American Heart Association (vol 121, pg e46, 2010).* Circulation, 2010. **121**(12): p. E260-E260.

6. Lloyd-Jones, D., et al., *Heart Disease and Stroke Statistics-2010 Update A Report From the American Heart Association.* Circulation, 2010. **121**(7): p. E46-E215.

7. Klabunde, R.E. *Ventricular and Atrial Hypertrophy and Dilation.* 2009.

8. Krum, H. and W.T. Abraham, *Heart failure.* Lancet, 2009. **373**(9667): p. 941-955.

9. Jessup, M., et al., *2009 Focused Update: ACCF/AHA Guidelines for the Diagnosis and Management of Heart Failure in Adults A Report of the American College of Cardiology Foundation/American Heart Association Task Force on Practice Guidelines.* Circulation, 2009. **119**(14): p. 1977-2016.

10. Frigerio, M. and E. Roubina, *Drugs for left ventricular remodeling in heart failure.* American Journal of Cardiology, 2005. **96**(12A): p. 10L-18L.

11. B. E. Jaski, J.K., S. Rademacher, L. Reardon, and D. Miller. *Heart Failure Online.* 2006; Available from: *http://www.heartfailure.org/eng_site/hf.asp.*

12. Stevenson, L.W., et al., *Left ventricular assist device as destination for patients undergoing intravenous inotropic therapy - A subset analysis from REMATCH (Randomized Evaluation of Mechanical Assistance in Treatment of Chronic Heart Failure).* Circulation, 2004. **110**(8): p. 975-981.

13. Najam, O., et al., *The Usefulness of Chronic Heart Failure Treatments in Chronic Cardiac Graft Failure.* Cardiovascular Therapeutics, 2010. **28**(1): p. 48-58.

14. Guyton, A.C., ed. *Textbook of Medical Physiology.* 8th ed. 1991, W.B. Saunders Company, p.77-78. 77-78.

15. Koeppen, B.M., Stanton B.A, ed. *Berne & Levy Physiology.* Sixth ed. Vol. Section IV. 2008, Mosby Elsevier, Section IV.

16. Curtis, M.W. and B. Russell, *Cardiac Tissue Engineering.* Journal of Cardiovascular Nursing, 2009. **24**(2): p. 87-92.

17. Simmons, C.R.E.a.C.A., ed. *Introductory Biomechanics, From Cells to Organism.* Chapters 2 and 4, ed. S.C. W.Mark Saltzman. 2007, Cambridge University Press. 18-98, 169-180.

18. Klabunde, R.E. *Ventricular Pressure-Volume Relationship.* 2009; Cardiovascular Physiology Concepts]. Available from: *http://www.cvphysiology.com/Cardiac%20Function/CF024.htm.*

19. Asanoi, H., et al., *Energetically optimal left ventricular pressure for the failing human heart.* Circulation, 1996. **93**(1): p. 67-73.

20. Karki, D.B., *Calculate left ventricular end diastolic pressure from Doppler Echocardiography.* Kathmandu University Medical Journal, 2006. **4, No.1**(13): p. 139.

21. Klabunde, R.E. *Signal Transduction Mechanism.* 2009; Available from: *http://www.cvphysiology.com/Blood%20Pressure/BP011.htm.*

22. Balnave, C.D., D.F. Davey, and D.G. Allen, *Distribution of sarcomere length and intracellular calcium in mouse skeletal muscle following stretch-induced injury.* Journal of Physiology-London, 1997. **502**(3): p. 649-659.

23. Klabunde, R.E. *Cardiac Moycytes and Sacromeres.* 2009; Available from: *http://www.cvphysiology.com/Cardiac%20Function/CF020.htm.*

24. Nishimura, S., et al., *Contractile dysfunction of cardiomyopathic hamster myocytes is pronounced under high load conditions.* Journal of Molecular and Cellular Cardiology, 2005. **39**(2): p. 231-239.

25. Klabunde, R.E. *Cardiac Excitation-Contraction Coupling.* 2009; Available from: *http://www.cvphysiology.com/Cardiac%20Function/CF022.htm.*

26. Klabunde, R.E. *Cardiac Muscle Force-Velocity Relationship.* 2009; Available from: *http://www.cvphysiology.com/Cardiac%20Function/CF006.htm.*

27. Yu, J.G. and B. Russell, *Cardiomyocyte remodeling and sarcomere addition after uniaxial static strain in vitro.* Journal of Histochemistry & Cytochemistry, 2005. **53**(7): p. 839-844.

28. Samarel, A.M., *Costameres, focal adhesions, and cardiomyocyte mechanotransduction.* American Journal of Physiology-Heart and Circulatory Physiology, 2005. **289**(6): p. H2291-H2301.

29. Kaneko, T., K. Kojima, and K. Yasuda, *Dependence of the community effect of cultured cardiomyocytes on the cell network pattern.* Biochemical and Biophysical Research Communications, 2007. **356**(2): p. 494-498.

30. de Bivort, B., S. Huang, and Y. Bar-Yam, *Dynamics of cellular level function and regulation derived from murine expression array data.* Proceedings of the National Academy of Sciences of the United States of America, 2004. **101**(51): p. 17687-17692.

31. Maron, B.J., *Hypertrophic cardiomyopathy.* Circulation, 2002. **106**(19): p. 2419-2421.

32.   Curl, C.L., et al., *Testosterone Modulates Cardiomyocyte Ca2+ Handling and Contractile Function.* Physiological Research, 2009. **58**(2): p. 293-297.

33.   Yeih, D.F., et al., *Temporal changes in cardiac force- and flow-generation capacity, loading conditions, and mechanical efficiency in streptozotocin-induced diabetic rats.* American Journal of Physiology-Heart and Circulatory Physiology, 2008. **294**(2): p. H867-H874.

34.   Gazmuri, R.J., M. Berkowitz, and H. Cajigas, *Myocardial effects of ventricular fibrillation in the isolated rat heart.* Critical Care Medicine, 1999. **27**(8): p. 1542-1550.

35.   Kummar, S., et al., *Phase 0 clinical trials: Conceptions and misconceptions.* Cancer Journal, 2008. **14**(3): p. 133-137.

36.   Marchetti, S. and J.H.M. Schellens, *The impact of FDA and EMEA guidelines on drug development in relation to Phase 0 trials.* British Journal of Cancer, 2007. **97**(5): p. 577-581.

37.   Tanaka, Y., et al., *Demonstration of a PDMS-based bio-microactuator using cultured cardiomyocytes to drive polymer micropillars.* Lab on a Chip, 2006. **6**(2): p. 230-235.

38.   Yang, Z.J., et al., *Rapid stimulation causes electrical remodeling in cultured atrial cells.* Biophysical Journal, 2003. **84**(2): p. 425A-425A.

39.   Parker, K.K., et al., *Myofibrillar architecture in engineered cardiac myocytes.* Circulation Research, 2008. **103**(4): p. 340-342.

40.   Kemi, O.J., et al., *Reduced pH and contractility in failing rat cardiomyocytes.* Acta Physiologica, 2006. **188**(3-4): p. 185-193.

41.   Bursac, N., et al., *Cardiomyocyte cultures with controlled macroscopic anisotropy - A model for functional electrophysiological studies of cardiac muscle.* Circulation Research, 2002. **91**(12): p. E45-E54.

42.   Camelliti, P., A.D. McCulloch, and P. Kohl, *Microstructured cocultures of cardiac myocytes and fibroblasts: A two-dimensional in vitro model of cardiac tissue.* Microscopy and Microanalysis, 2005. **11**(3): p. 249-259.

43.   McDevitt, T.C., et al., *In vitro generation of differentiated cardiac myofibers on micropatterned laminin surfaces.* Journal of Biomedical Materials Research, 2002. **60**(3): p. 472-479.

44.   Park, J., et al., *Mechanotransduction of cardiomyocytes interacting with a thin membrane transducer.* Journal of Micromechanics and Microengineering, 2007. **17**(6): p. 1162-1167.

45.   Feinberg, A.W., et al., *Muscular thin films for building actuators and powering devices.* Science, 2007. **317**(5843): p. 1366-1370.

46.   Gwak, S.J., et al., *The effect of cyclic strain on embryonic stem cell-derived cardiomyocytes.* Biomaterials, 2008. **29**(7): p. 844-856.

47.   Gupta, V. and K.J. Grande-Allen, *Effects of static and cyclic loading in regulating extracellular matrix synthesis by cardiovascular cells.* Cardiovascular Research, 2006. **72**(3): p. 375-383.

48.   Park, J.Y., et al., *Micro pumping with cardiomyocyte-polymer hybrid.* Lab on a Chip, 2007. **7**(10): p. 1367-1370.

49.   Tanaka, Y., et al., *An actuated pump on-chip powered by cultured cardiomyocytes.* Lab on a Chip, 2006. **6**(3): p. 362-368.

50.   *Bradycardia (Slow Heart Rate) - Overview.* 2009; Available from: *http://www.webmd.com/heart-disease/tc/bradycardia-slow-heart-rate-overview.*

51.   Burstein, B., et al., *Atrial cardiomyocyte tachycardia alters cardiac fibroblast function: A novel consideration in atrial remodeling.* Cardiovascular Research, 2007. **76**(3): p. 442-452.

52.   Hung, C.T. and J.L. Williams, *A METHOD FOR INDUCING EQUI-BIAXIAL AND UNIFORM STRAINS IN ELASTOMERIC MEMBRANES USED AS CELL SUBSTRATES.* Journal of Biomechanics, 1994. **27**(2): p. 227-232.

53.   Schaffer, J.L., et al., *DEVICE FOR THE APPLICATION OF A DYNAMIC BIAXIALLY UNIFORM AND ISOTROPIC STRAIN TO A FLEXIBLE CELL-CULTURE MEMBRANE.* Journal of Orthopaedic Research, 1994. **12**(5): p. 709-719.

54.   Kim, H.J., et al., *A Biaxial Stretchable Interconnect With Liquid-Alloy-Covered Joints on Elastomeric Substrate*. Journal of Microelectromechanical Systems, 2009. **18**(1): p. 138-146.

55.   *Material: PDMS (polydimethylsiloxane)*. 6.777J/2.751J Material Property Database; Available from: *http://www.mit.edu/~6.777/matprops/pdms.htm*.

56.   *Health Encyclopedia - Diseases and Conditions*. 2009, USA Today.

57.   Pimentel, D.R., et al., *Reactive oxygen species mediate amplitude-dependent hypertrophic and apoptotic responses to mechanical stretch in cardiac myocytes*. Circulation Research, 2001. **89**(5): p. 453-460.

58.   Liao, X.D., et al., *Mechanical stretch induces mitochondria-dependent apoptosis in neonatal rat cardiomyocytes and G(2)/M accumulation in cardiac fibroblasts*. Cell Research, 2004. **14**(1): p. 16-26.

59.   White, F.M., ed. *Fluid Mechanics*. 2008, McGraw-Hill Companies, Inc. Pg. 25-26. pg. 25-26.

60.   Hescheler, J., et al., *MORPHOLOGICAL, BIOCHEMICAL, AND ELECTROPHYSIOLOGICAL CHARACTERIZATION OF A CLONAL CELL (H9C2) LINE FROM RAT-HEART*. Circulation Research, 1991. **69**(6): p. 1476-1486.

61.   Simmerman, H.K.B. and L.R. Jones, *Phospholamban: Protein structure, mechanism of action, and role in cardiac function*. Physiological Reviews, 1998. **78**(4): p. 921-947.

62.   MacLennan, D.H. and E.G. Kranias, *Phospholamban: A crucial regulator of cardiac contractility*. Nature Reviews Molecular Cell Biology, 2003. **4**(7): p. 566-577.

APPENDIX

A. CHARACTERIZATION OF MEMBRANE THICKNESS

The thickness of the membrane was measured using Profilometer Veeco Dektek 8M. To obtain different thicknesses, 6 different spinning speeds (200 rpm, 700 rpm, 1000 rpm, 2500 rpm, 4000 rpm, and 5000 rpm) were performed. For each spinning speed, two different PDMS mixtures (ratio 10:1 w/w) were made at different times. To measure the thickness of the PDMS membrane, two or three different locations of the PDMS membrane (the edges, the center) on the silicon wafer were measured. Then, the average value for each set was calculated as well as the standard deviation (Table A and Fig. A)

Table A. Membrane thickness obtained at different spinning speeds.

Spin Speed	Membrane thickness							average thickness	STDEV
rpm	μm	μm	μm	μm	μm	μm	μm	μm	μm
200	491.21	488.41	514.54	513.55	530.53	455.37	506.66	500.04	24.41
700	136.84	138.89	137.04	151.13	132.97	133.99	131.3	137.45	6.58
1000	94.48	94.38	92.76	93.83	83.13	91.07	92.64	91.76	3.98
2500	35.49	35.29	38.84	36.08	35.99	34.68	34.8	35.88	1.41
4000	20.41	20.93	22.26	23.3	22.37	21.55	20.24	21.58	1.13
5000	18.03	16.71	16.54	17.86	16.04	16.73	16.48	16.91	0.74

$y = 130728x^{1.05}$
$R^2 = 0.9999$
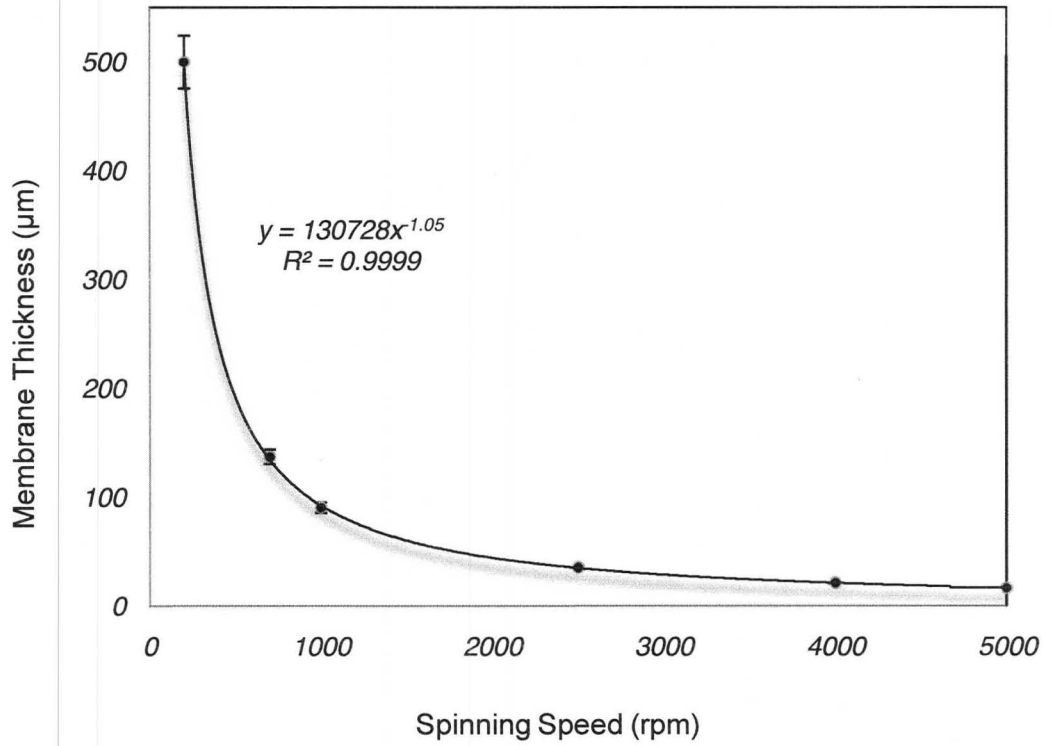
<u>Figure A.</u> Membrane thickness as function of spinning speed

B. PUMP FLOW RATE CHARACTERIZTION

To know accurately the flow rate delivered by the peristaltic pump for different tubing diameter, the pump was calibrated. To calibrate the pump, a flow rate value was set on the digital display of the pump and the volume delivered in 30 seconds was measured. For each flow rate set on the pump, four measurements of the volume were performed. (Table B and Figure B).

<u>Table B</u>. Raw data for the flow rate corresponding to the digital number on the peristaltic pump

Number on pump	Flow rate 1st	Flowrate 2nd	Flowrate 3rd	Flowrate 4th	Average flowrate	Standard Deviation
	mL/30sec	mL/30sec	mL/30sec	mL/30sec	mL/30sec	mL/30sec
40	4.350	4.275	4.400	4.245	4.318	0.071
50	5.273	5.052	5.250	5.104	5.170	0.108
60	6.220	5.895	6.080	5.626	5.955	0.257
70	7.305	6.955	7.133	6.853	7.062	0.199
80	8.092	7.604	8.088	7.438	7.806	0.335
90	9.162	8.567	9.021	8.380	8.783	0.369
100	10.077	9.503	9.920	9.272	9.693	0.371
110	10.488	9.872	10.721	10.224	10.326	0.365
120	11.314	10.892	11.677	11.125	11.252	0.332
130	12.900	12.400	12.600	12.100	12.500	0.337
140	13.511	12.864	13.422	12.479	13.069	0.487

$y = 0.0885x + 0.7532$
$R^2 = 0.9983$

Flow rate set on the digital display
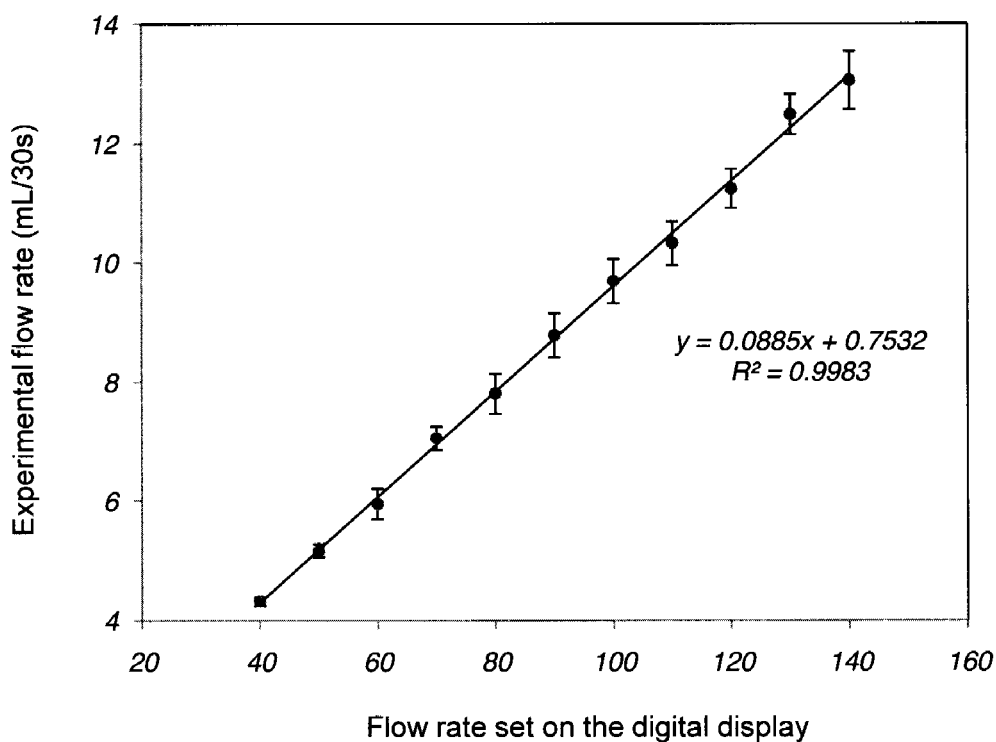
<u>Figure B</u>. Flow rates as a function of frequency.

C. CELL CULTURE MEDIUM AND SOLUTIONS

C.1. 1X PBS (Phosphate Buffered Saline solution)

For 1L of 1X PBS solution:

- 900 mL of de-ionized water (DI water)

- 100 mL of 10X PBS, pH 7.4 (Fisher Scientific, BP399-1)

- Mix well and filter with 0.02 μm filter

- Store at room temperature

C.2. 1X Trypsin Solution

For 100 mL of 1X Trypsin solution:

- 90 mL of sterilized 1X PBS

- 10 mL of 10X Trypsin (MP Biomedicals, 1689349)

- Mix well and store at 4 °C, if used in less than 1 month, or at -20 °C

C.3. 0.02% gelatin solution

For 100 mL of 0.02% Gelatin Solution:

- 100 mL of DI water

- 2.0 mg of gelatin (BD Biosciences, Cat # 214340)

- Heat at 121 °C in the autoclave for 15 min

- Cool and filter.

- Store at 4 °C

C.4. Extracellular matrix solution (ECM solution)

For 50 mL of ECM solution:

- 42.5 mL of 0.02% filtered Gelatin Solution

- 5.0 mL of Attachment Factor Solution (Genlantis, Cat # PR123100)

- 2.5 mL of 1.0 mg /mL Fibronectin solution* (BD Biosciences, 356008)

- Mix well, aliquot into 15 mL tubes and store at -20 °C

* Note: reconstitute 5 mg of Fibronectin in DI water to obtain 1 mg /mL
fibronectin, and dissolve it slowly without agitation, store at -20 °C)

C.5. H9c2 cell culture medium

For 555 mL H9c2 cell culture medium:

- 500 mL of Dulbeco's Modified Eagles' Medium (DMEM) (Cellogro, Cat#10-013 CV).

- 55 mL of Hyclone@ Fetal Bovin Serum (FBS) (ThermoScientific, Cat# SV30014-03)

- 5.5 mL of Antibiotic Penicillin-Streptomycin Solution (Cellgro, Cat# 30-002-CI)

- Mix well and store at 4 °C

C.6. 4% PFA solution (Paraformaldehyde solution)

For 40 mL 4% PFA solution:

- 30 mL of 1X PBS solution

- 10 mL of 16% Formaldehyde Solution (Thermo Scientific, 28908)

- Mix well and store at 4 °C

C.7. Washing buffer (0.05% Tween-20 solution)

For 100 mL of washing buffer:

- 99.95 mL of 1X PBS solution

- 0.05mL Tween-20 (Fisher Scientific, BP 337-100)

- Mix well and store at 4 °C

C.8. 0.1% Triton X-100 solution

For 100 mL of 0.1% TritonX-100 solution:

- 99.9 mL of 1X PBS solution

- 0.1 mL of Triton X-100 (Fisher Scientific, BP-151-500)

- Mix well and store at 4 °C

C.9. Blocking solution, 0.5% Bovine Serum Albumin (BSA) solution

For 50 mL of blocking solution:

- 50 mL of 1X PBS solution

- 0.25 g of BSA (Sigma, A9418-10g)

- Mix well, filter, and store at 4 °C

C.10 0.05% Sapronin solution

For 10 mL of 0.05% sapronin solution:

- 10 mL of 1X PBS solution

- 5.0 mg of sapronin

- Mix well, store at 4 °C and use it within a week

D. CELL CULTURE PROTOCOLS

D.1 Sterilization

a. The platform, collapsible valve and tunable valve:

- Soak the parts in 10% hydrochloride for 10 minutes

- Rinse well with tap water for 1 minute and dry with tissue

- Soak in 70% isopropanol for 10 min in the hood and keep the parts

under sterile conditions

- Rinse with 1X sterilized PBS before used

b. The tubes, needles, medium containers:

Autoclave at 121 °C for 15 min

c. Digital Manometer:

- Remove all old medium inside

- Fill with 70% isopropanol for at least 10 minutes

- Remove all the isopropanol and refill with filtered 1X PBS

- Remove all 1X PBS and refill fully with filtered 1X PBS

d. Tensile ring and the reservoir:

- Wash with water and let it air dry.

- Use clear tape to remove the particle dust

- Rinse with 70% isopropanol then heat on the hot plate at 115 °C for 10 minutes

- Keep it in sterile conditions

e. The cell culture chamber:

Oxygen plasma and heat at 115 °C (after bonding) was applied

D.2   Cell culture

Cells were grown in a 25 mL cell culture flask and split when they were 90-100% confluence. All manipulations must be performed inside the cell culture hood.

- Warm the medium at 37 °C and spray the bottle with 70% isopropanol before placing it inside the cell culture hood.

- Under a microscope, check if the cells are confluent, contaminated (clear or cloudy, tiny particles), and shape of cells. Then transfer the cell culture flask to the cell culture hood

- Remove the old cell culture medium

- Wash with 5 mL of filtered 1X PBS solution, gently swirl and then remove the PBS

- Add 3 mL of 1X Trypsin, shake gently, and incubate at 37°C for 4-5 mins to detach the cell. To detach the cells faster, tap the bottom of the flash few times after the incubating period

- Neutralize trypsin with 10 mL fresh H9c2 cell culture medium. Pipette up and down two or three times gently. Then, transfer all cell suspended solution into a 15 mL centrifuge tube.

- Centrifuge at 1000 rpm for 5 minutes at 25 °C.

- Discard the supernatant and keep the cell pellet

- Re-suspend the cell pellet with 4 mL fresh cell culture medium.

- Add 5 mL of medium to the cell culture flash and transfer 0.5 mL of cell suspended solution to the flash. Mix one or two times with pipette.

- Incubate in cell culture incubator (37 °C, 5% CO_2) and change cell culture medium for every two or three days.

- If planning to do the experiment, keep the remaining of cell suspended solution for the experiment (see Appendix D.4). Otherwise bleach and discard the cell suspended solution.

- Clean up the hood with 70% isopropanol

D.3. Preparation of the cell culture chamber

Two or three days before seeding the cell on the thin PDMS membrane in a cell culture chamber of the device, the membrane must be coated with ECM substrate for the cell to attach and grow.

- Apply oxygen plasma (10% oxygen, 100 mmTorr, and 100 mmHg) on the membrane for 1 minute

- Insert a 18G needle into the channel

- Insert the sterilized tensile ring into the chamber

- Place the sterilized reservoir on the top of the chamber and press it

- Add 100 µl of ECM solution.

- For sterilization, apply UV light for 4 minutes.

- Store the chambers at 4 °C. for 3 days

- For cell culture, incubate the chambers at 37 °C for 30 min

D.4. Seed cells in the cell culture chamber

- Count the cells to estimate the total number of cells per mL.

- Use the formula $C_1V_1 = C_2V_2$ to calculate the volume needed to have 2.5×10^4 cells per chamber

- Transfer the coated ECM cell culture chambers from the incubator to the hood.

- Remove the ECM solution and quickly fill the chamber with 200 µL of cell culture medium

- Remove 125 µL of medium from the chamber

81

- Add 2.5 x 10^4 cells suspended in medium into each well

- Observe the cells under the microscope. If the cells are not distributed

homogeneously, then pipette gently up and down two or three times

- Incubate for 4 h or until the cells attach and spread

- Fill the reservoir with H9c2 cell culture medium (~1.3 to 1.5 mL).

- Incubate at 37 °C. After 1 h, observe the devices and ensure there is not

leakage

- Culture the cells for 48 h at 37 ^{0}C

- Change medium every 24 h

D.5. Cell counting and calculation of cell concentration with the use of a Cellometer® (Nexcelom Bioscience, CP2-002):

- Add 20 μL of cell suspension into a sample introduction port of the counting

chamber and wait for one minute.

- Place Cellometer® under an optical microscope and adjust the microscope to

visualize the grid line and the cells.

- Count cells as indicated by the manufacturer. Briefly, count the cells within four

large squares. For each square, count the cells inside the square plus the cell

attaching the upper and right edges.

- Calculate the cell concentration

The average cells/square = (1/4) x (total cells counted in 4 squares)

Cell concentration (cells /mL) = 10^4 x (average cells /square)

D.6 Immunofluorescence staining

All the solutions must be warmed at 37 °C or at room temperature. For each cell chamber:

- Fixed the cells with 200 μL of warmed 4% PFA solution for 20 mins at RT.

- Wash two times with the warmed washing buffer (250 μL /chamber each time)

- Permeabilize with 250 μL of 0.1% Triton X-100 solution for 5 mins at RT.

- Washed two times with washing buffer ((250 μL /chamber each time)

- Block with 250 μL blocking solution for 30 mins at RT

- Incubate on a low speed shaker with the primary antibody p-phospholamban (Ser 16, 1:100; Santa Cruz Biotechnology, Santa Cruz, CA) in freshly made 0.05% BSA solution at RT for 1 h

- Wash three times with washing buffer for 5 mins each time at RT

- Incubate on a low speed shaker at RT for 60 min with the second antibody, FITC-conjugated chicken anti-goat (1:100; Alexa Fluor 488, Invitrogen, Carlsbad, CA) in 0.05% BSA solution. To avoid quenching of the fluorescence dye, cover the chamber with aluminum with foil.

- Wash three times with washing buffer, 5 mins each time at RT

- For F-actin detection, incubate at RT for 1 h with TRITC-conjugated Phalloidin (1:100; Millipore, Billerica, MA) in blocking buffer.

- Wash three times with washing buffer

- Add 250 μL of Light Diagnostics mounting fluid (Millipore, Billerica, MA)

- Examine the cells using a Nikon Eclipse TE2000-U fluorescence microscope, 20X.

E. PROGRAM OF THE HEADWAY SPINNER

This program is set up to make PDMS membrane at 400 rpm

- On the program panel, select "Recipe", then enter a program number.

- Press "Step", enter 1, then:

  - Press "Step terminate", enter 0.5 sec, press "Enter".

  - Press the 'Speed/Ramp', enter 200 rpm, press "Enter"

  - Press the "Speed/Ramp" again, enter 100 rpm, press "Enter" Press "Step", enter 2

  - Press the "Terminate", enter 30 sec, press "Enter"

  - Press the "Speed/Ramp", enter 400 rpm, press "Enter"

  - Press the "Speed/Ramp" again, enter 200 rpm, press "Enter"

- Press "Step", enter 3

  - Press the "terminate", enter 0.5 sec, press "Enter"

  - Press the "Speed/Ramp", enter 200 rpm, press "Enter"

  - Press the "Speed/Ramp" again, enter 100 rpm, press "Enter"

- Press "Step", enter 0 to exit the program. The system is ready to run.

F. PROTOCOL TO MAKE THE PDMS THIN MEMBRANE

- Programming the Headway Spinner as Appendix E.

- Place the wafer on the center of the platform of the spinner and press "Vacuum" on the program panel.

- Check the balance of the wafer by spinning the wafer.

- Add PDMS on the center of the wafer (~ 5 g or as large as a dollar coin).

- Close the lid.

- Press the green button on the control paddle to start the spinning.

- Wait until the spinner completely stops, open the lid, turn off the vacuum, and transfer the PDMS coated wafer to the hot plate.

- Bake at 115 °C for 10-15 min, then, cool down the wafer at room temperature.

G. OPERATING THE μCCCM SYSTEM

- Turn on the peristaltic pump

- Set 15 flow rate on the display of the pump and circulate fluid for 15 min

- Increase the flow rate by 10 on the pump every 10 min to reaches 40 on the digital display. Circulate fluid for another 10-15 min.

- To start the pressure generator, turn on the air supply, then the pulsatile pressure generator and wait ~1 min. Set the pulsatile pressure generator to 80 bpm and 50% systolic.

- To monitor the pressure, turn on the digital manometer connected to the cell chamber

- Let the system run for 15 min.

- Increase the pressure in the pressure generator to 15mmHg, then every 15 minutes, increase the pressure by 15mmHg until it reaches 45mmHg.

- Tighten gently the tunable valve to increase pressure slowly.

- Adjust the tunable valve and pressure generator to obtain the desired pressure.

Every time the pressure is adjusted, wait for 10-15 min for pressure stabilization.

Note: the pressure generator and tunable valve must be adjusted alternatively to set the pressure. When tighten the tunable valve, if the lower pressure is higher than 30mmHg, increase the pressure in the pressure generator. If the lower pressure has negative values, reduce the pressure in the generator. If the peak pressure increases suddenly, release the tunable valve.

- To stop the system, first, slowly release the tunable valve. Then, reduce the pressure in the pressure generator gradually all the way to 0mmHg, within30 min. Then, turn off the air supply system. Wait for 5 min, then, turn of the pressure generator. Reduce flow rate and stop the circulation of fluid.

H. LIST OF ABBREVIATIONS

bpm	Beats per minute
BSA	Bovine Serum Albumin
cAMP	cyclic Adenosine Monophosphate
CB	Cork Borer
CNC	Computer Numerical Control
CVD	Cardiovascular disease
d	Diameter
DI water	De-ionized water
DMEM	Dulbeco's Modified Eagles's Medium

ECM	Extra-cellular maxtrix
FBS	Fetal Bovine Serum
HF	Heart Failure
ID	Inner diameter
IP3	Inositol Triphosphate
l, L	Length
LV	Left ventricle
LVAD	Left ventricle assistant device
L_0	Length between two black dots at 0.0 mmHg
L_f	Length between two black dots after pressure is applied
mL	Milliliter
OD	Outer diameter
PBS	Phosphate Buffer Saline
PDMS	Polydimethyl siloxane
PFA	Paraformaladehyde
RIE	Reactive Ion Etcher
rpm	revolution per minute
τ	Shear stress
μ	Viscosity
μCCCM	Microfluidic cardiac cell culture model

CURRICULUM VITAE

Education:

08/2008- present	The University of Louisville, KY
	Pursuing a master of science in department of mechanical engineering
	GPA: 3.83/4.0
08/1995- 08/1999	The University of Oklahoma, OK
	BS in Chemical Engineering/ Biotechnology Option
	GPA: 3.75/4.0
08/1993- 08/1995	Oklahoma Community College, OK
	Pre-Pharmacy
	GPA: 3.8/4.0

Professional Experience:

05/2007- present	Graduate Student Research Assistant- Dr. P. Sethu
	Department of Bioengineering/Mechanical Engineering, UofL
	Design and fabrication of micro-electro-mechanical systems (MEMS) devices for cardiovascular research and flow cytometry
08/2005-05/2007	Research Technologist II- Dr. B. Clark
	Department of Biochemistry & Molecular Biology, UofL.
	The effects of Bt_2cAMP on the expression of COUP-TF, STAR, and SF-1 in diabetic diseases.
08/2004- 08/2005	Research Technologist II - Dr. P. Feldhoff and Dr. H. Lassiter
	Department of pediatrics and neonatology, UofL
	The regulation of C_3 and C_9 in stroked infant rat brain
11/1999- 06/2003	Research Assistant- Dr. L. Griffith
	Department of Neuroscience and Biochemistry,
	Brandeis University, MA
	The effect of Eag Potassium Channel on Calcium/ Calmodulin Dependent Protein Kinase II Po

08/ 1998- 05/1999   Research Volunteer
                      Department of Biochemical Engineering, the University of
                      Oklahoma, OK
                      Separation of phenol from waste water streams

Publications in Journals and Conference Proceedings:

Mai-Dung Nguyen, Guruprasad Giridharan, Sumanth D. Prabhu, and
Palaniappan Sethu, "Microfluidic Cardiac Circulation Model for Functional
Cardiomyocyte Studies." Engineering in Biology and Medicine Conference Sept
2, 2009, Minneapolis, MN

William N. White, Ashok Raj, Mai-Dung Nguyen, Salvatore J. Bertolone, and
Palaniappan Sethu, "Clinical application of microfluidic leukocyte enrichment
protocol in mild phenotype sickle cell disease (SCD)." Biomed Microdevices
(2009) 11:477-483

Mai-Dung Nguyen, Buruprasad Giridharan, Palaniappan Sethu, "Cardiomyocyte
Acutuator for Microfluidics Platform Nozzle-Diffuser Pump." Poster
presentation, MicroTAS 2008, October- Twelfth International Conference on
Miniaturized System for Chemistry and Life Science, San Diego, CA

William White, Mai-Dung Nguyen, and Palaniappan Sethu, "Microfluidics
enumeration protocol for comprehensive profiling of nucleated cells in mild
phenotype sickle cells disease (SCD)." Poster presentation, MicroTAS 2008,
October- Twelfth International Conference on Miniaturized System for Chemistry
and Life Science, San Diego, CA.

Bobby L. Gibbons, Mai-Dung Nguyen, Guruprasad Giridharan, Mohammed
Ishmahil, Sumant D. Prabhu and Palaniappan Sethu, "Microfluidic Platform to
Study Cardiomyocyte Mechanotransduction", Research Louisville! 2008,
Louisville, KY. (2nd Place, Interdisciplinary Research Category)

William N. White, A. Raj, Mai-Dung. Nguyen, S.J. Bertolone and Palaniappan
Sethu, "Comprehensive profiling of leukocytes and circulating endothelial cells in
asymptomatic SCD using microfluidic isolation", ASPHO 2008, Cincinnati, OH,
February 2008.

Mai-Dung. Nguyen, William N. White, Guruprasad Giridlaran, and Palaniappan
Sethu, "Cardiomyocyte Actuator", Internal Poster Competition of Engineering
Department, UofL, 3, 2008
Lori A. Devlin, Mai-Dung Nguyen, et. al. Effects of endotoxin administration
and cerebral hypoxia-ischemia on complement activity and local transcriptional

regulation in neonatal rats. Neuroscience Letters, Vol. 390, Issue 2, December 23, 2005, p. 109-113.

Xiu Xia Sun, James J.L Hodge,Yi Zhou, Mai-Dung Nguyen, and Leslie C. Griffith. The Eag Potassium Channel Binds and Locally Activates Calcium/ Calmodulin Dependent Protein Kinase II. The Journal of Biological Chemistry, Vol. 279, No. 11, March 12, 2004, p. 10206-10214.

Honors and Affiliations:

2010- present	Member of Bioengineering Society
2009-present	Member of the Society of Engineering Women
1998	Member of the Best Group in Laboratory Chemical Engineering Advanced Design
1999	Second place for team work with the Senior Design Project of Energy Retrofit
1996-1997	Passage to Progress (PTP) Scholarship
1995-1999	Dean's List Honor Roll at the University of Oklahoma, OK
1994-1999	Member of Phi Thepa Honor, Golden Key Honor, and Tau Beta Pi Society.
1993-1995	President's Honor Roll at Oklahoma City Community College, OK

Community Services:

10/2005-present	St. JOHN VIANNEY CHURCH, KY *Catechism teaching*
01/2007-11/2007	BAPTIST EAST HOSPITAL, KY *Pastoral care ministry*
05, 2007	NEW ORLEAN, LA *Katrina Recovery.*
10/1999-06/2003	St. WILLIAM CHURCH, MA *Catechism teaching*